

# Matrix Profile XXIV: Scaling Time Series Anomaly Detection to Trillions of Datapoints and Ultra-fast Arriving Data Streams

Yue Lu<sup>1</sup>, Renjie Wu<sup>1</sup>, Abdullah Mueen<sup>2</sup>, Maria A. Zuluaga<sup>3</sup>, Eamonn Keogh<sup>1</sup>

<sup>1</sup> *University of California, Riverside, Riverside, USA*

<sup>2</sup> *Department of Computer Science, University of New Mexico, Albuquerque, USA*

<sup>3</sup> *Data Science Department, EURECOM, Sophia Antipolis, France*

{ylu175, rwu034} @ucr.edu, mueen@cs.unm.edu, maria.zuluaga@eurecom.fr, eamonn@cs.ucr.edu

**Dear Reader: This is an expanded version of the 2022 SIGKDD paper.**

**Abstract**— Time series anomaly detection is one of the most active areas of research in data mining, with dozens of new approaches been suggested each year. In spite of all these creative solutions proposed for this problem, recent empirical evidence suggests that the *time series discord*, a relatively simple twenty-year old distance-based technique, remains among the state-of-art techniques. While there are many algorithms for computing the time series discords, they all have limitations. First, they are limited to the batch case, whereas the online case is more actionable. Second, these algorithms exhibit poor scalability beyond tens of thousands of datapoints. In this work we introduce DAMP, a novel algorithm that addresses both these issues. DAMP computes exact left-discords on fast arriving streams, at up to 300,000 Hz using a commodity desktop. This allows us to find time series discords in datasets with trillions of datapoints for the first time. We will demonstrate the utility of our algorithm with the most ambitious set of time series anomaly detection experiments ever conducted. We will further show that our speedup improvements can be applied in the multidimensional case.

**Keywords:** *Time Series, Anomaly Detection, Streaming Data*

## 1 INTRODUCTION

Time series anomaly detection is one of the most important and widely used tools investigated by the data mining community [2][14][21]. It can be applied offline to investigate archival data, or online, to monitor critical situations where human intervention is possible. For example, by summoning a doctor or shutting down a machine that may be about to damage itself. Given its importance, it is unsurprising that this area attracts a lot of attention from the community, with dozens of algorithms

proposed each year. However, in spite of the plethora of algorithms in the literature, there is increasing evidence that a twenty-year-old distance-based method called *time series discords* is still competitive [21]. Discords are competitive with deep learning methods in spite (or perhaps *because*) of their great simplicity. A time series discord is simply the subsequence of a time series that is maximally far from its nearest neighbor. At least one-hundred papers have reported using discords to solve problems in diverse domains, and discords seem to be the only time series anomaly detection technique to produce “superhuman” results (see discussion in Section 2). However, discords have three important limitations that have limited their broader adoption:

- If an anomalous pattern appears at least twice in the time series, then each occurrence will be the other nearest neighbor, and thus fail to optimize the discord definition. This is informally called the *twin-freak* problem.
- Discords are only defined for the *batch* case, but anomaly detection is most actionable in *online* settings.
- In spite of extensive progress in speeding up discord discovery, datasets with millions of datapoints remain intractable.

In this paper we introduce DAMP (Discord Aware Matrix Profile), a novel algorithm which solves all the above problems.

- DAMP is not confused by repeated anomalies (twin-freaks), it simply flags the first occurrence (if desired, other occurrences can then be found by simple similarity search).
- DAMP is defined for both online and offline cases. Moreover, DAMP has an extraordinary fast throughput, exceeding 300,000 Hz on standard hardware.
- As the previous bullet point suggests, DAMP is extraordinarily scalable. For the first time, this allows us to consider datasets with millions, billions and even trillions of datapoints.

The rest of this paper is organized as follows. In Section 2 we motivate the use of *discords* as the time series anomaly definition most worthy of acceleration and generalization. We also concretely define a new term, *effectively online*, that allows DAMP to tackle ultra-fast real-time data sources found in industry and science. Section 3 contains the necessary definition and notation required, and Section 4 discusses

related work, before we introduce our algorithm in Section 5. In Section 6 we conduct the most ambitious empirical evaluation of time series anomaly detection ever attempted.

## 2 MOTIVATION

Before we continue, it is necessary to answer the following question. Why do we attempt to fix discord’s scalability issues instead of inventing a new algorithm, or making one of the many dozens of more recently proposed methods more scalable?

The reason is that there is increasing evidence that discords remain competitive with the state-of-the-art<sup>1</sup> [21]. Among the hundreds of time series anomaly detection algorithms proposed in the last two decades, only time series discords could claim to have been adopted by more than one hundred independent teams to actually solve a real-world problem. For example, a group of climatologists at France’s UMR Espace-Dev laboratory use discords to find anomalies in climate data [17]. A team of researchers at NASA’s JLP lab have applied discord discovery to planetary data, noting that “(discords) *detect Saturn bow shock transitions well*” [9]. A group based in Halmstad University created a tool called IUSE for applying discord discovery to industrial datasets. One of their first applications was to a City Bus Fleet dataset, where they noted that the discords discovered did indeed have an objective meaning “*The discords in this case primarily consisted of significant drops of pressure ... likely correspond to the drainage of the wet tank.*” [24]. Finally, a team of researchers at the National Renewable Energy Laboratory, in Golden, Colorado, have used discords to find anomalies in a large building portfolio, showing that they could discover anomalies with diverse causes caused by both “*internal (occupant behavior) and external factors (weather conditions).*” [28]. There are several other time series anomaly detection algorithms that are well cited [14][30], but most of the citations are from rival methods comparing these algorithms on a handful of benchmarks [35], there is little evidence that anyone actually uses these algorithms to solve real-world problems.

In addition, time series discords seem to be the only anomaly detection algorithm that has been demonstrated to perform at superhuman levels [21]. All other algorithms that

---

<sup>1</sup> Note that some papers misattribute the success of their anomaly detection to the Matrix Profile or to HOTSAX, but these are simple different algorithms to compute time series discords.

we are aware of have shown to discover anomalies that are also readily apparent to the human eye. For example, a recent paper proposed an LSTMs network for anomaly detection and evaluated it on data retrieved from Mars [14]. However, the only anomaly shown in the paper shows a visually obvious anomaly where a repeated periodic pattern suddenly transitions to a literal flatline. Of course, this does not mean that such algorithms have no value, as human attention is very expensive. However, the literature also offers some examples where discords have found anomalies that are very subtle, defying the possibility of human discovery. For example, in [21], their Figure 8 and Figure 9 both seem to meet that criterion. For completeness, we will show some additional examples. Consider Fig. 1, which shows the vibration of an industrial motor [7][23].

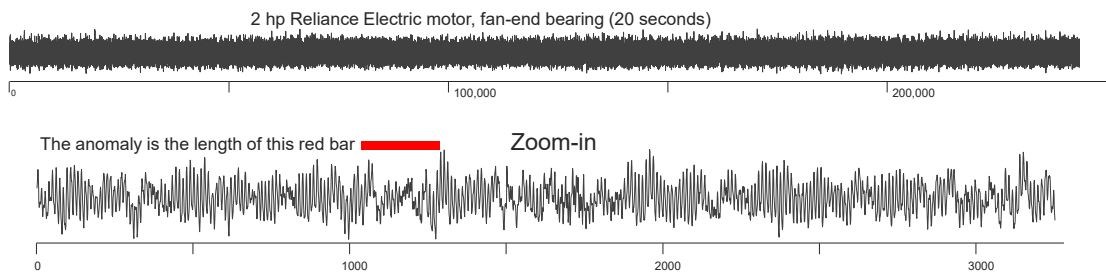


**Fig. 1** *top*) A 20-second run of an industrial motor. *bottom*) a zoom-in of the region known to contain an anomaly, which is the length of (but not necessarily at the location of) the red bar.

The data comes for a motor running under no load, however for a brief instant a load was applied and immediately removed, creating an anomaly. It is clearly fruitless to visually search for the anomaly in the *full* dataset, however, even if we zoom into a local region containing the anomaly, it is not clear where it is. In Fig. 2 we task time series discords with detecting the anomaly.

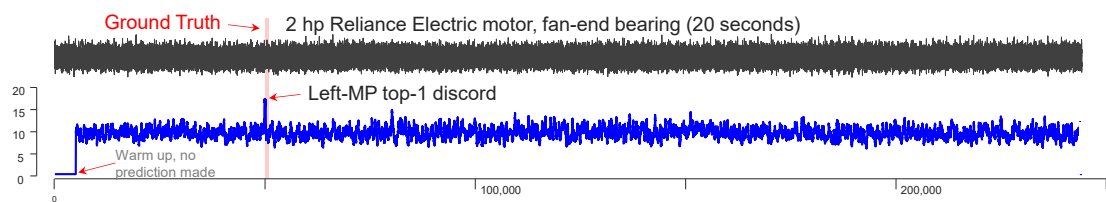


**Fig. 2** *top*) A 20-second run of an industrial motor. *bottom*) The time series discord discovered by the Left-MP correctly locates the anomaly. Note that higher values are more anomalous.

Beyond the accuracy of discords prediction here, note that this dataset contains 244,189 datapoints, representing about 20 seconds of wall clock time recorded at 12,000 Hz.

We are not aware of any anomaly detection algorithm in the literature that could process this dataset in real-time, however, as we will show, DAMP *can*.

We also consider a dataset that is dramatically different to the bearing data. In Fig. 3 we show the Left-MP for an ECG which we know contains a single anomaly beat, a *ventricular contraction*.

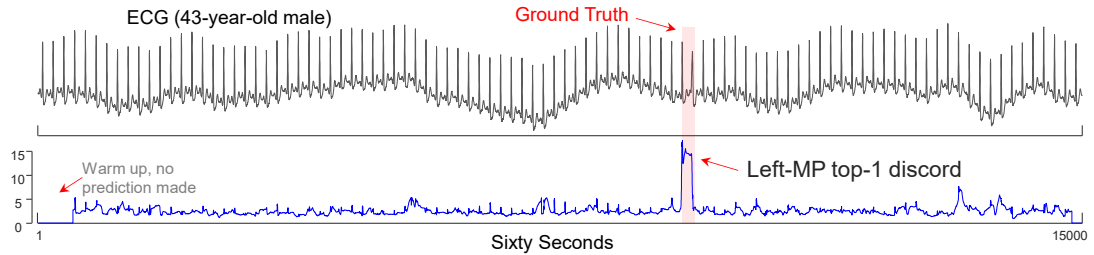


**Fig. 3** *top*) A sixty-second snippet of an ECG. *bottom*) The top-1 time series discord correctly locates the anomaly.

This dataset has a wandering baseline which is diagnostically meaningless, but which distracts the human eye (and many algorithms). However, once again time series discords have no problem detecting the anomaly, which noted cardiologist Dr. Gregory Mason says is on the cusp of his ability to detect by eye.

Finally, in Fig. 4 we consider a dataset that was explicitly created with the sole purpose of having anomalies that are “*difficult to spot for the human eye*” [31]. Here again discords are superhuman.

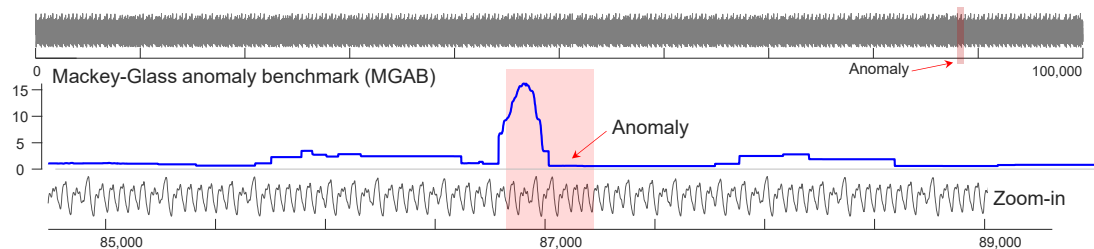


**Fig. 4** *top*) The MGAB dataset was built to defy visual discovery of anomalies. *bottom*) The Top-1 time series discord correctly locates the anomaly.

In summary, both the recent literature and our experiments suggest that time series discords are *at least* competitive with recently proposed algorithms, and thus worthy of accelerating to allow discords to be discovered in settings that are currently infeasible.

## 2.1 Effectively Online Anomaly Detection

Although the meaning of the terms *batch* and *online* are obvious, it is helpful to introduce a new term, *effectively online*, to make our claim clearer. A true online

algorithm reports the instant it detects a monitored condition. However, let us imagine the following scenario: After a difficult cardiac surgery, a doctor decides she wants to monitor her patient for anomalous heartbeats, which may be an indication of postoperative Cardiac Tamponade (CT). If the patient does have an ECG suggestive of CT symptoms, the doctor has perhaps eight to ten minutes to confirm CT with an ultrasound and perform pericardiocentesis, a procedure done to remove fluid that has built up in the sac around the heart [18]. Because the doctor is nervous about the possibility of CT, she arranges the rest of her day such that she can be in the ICU within two minutes, for example eating her lunch in a hospital cafeteria rather than her favorite restaurant across town. Clearly in this situation an algorithm that reported an anomalous heartbeat ten minutes after its appearance would be unacceptable. However, an algorithm that reported an anomalous heartbeat at most two seconds after it appears would be just as good as a true online algorithm. As such we propose the following definition:

**Definition 1:** An algorithm is said to be *effectively online*, if the lag in reporting a condition has little or no impact on the actionability of the reported information.

Note that the scale of the permissible lag is problem dependent. In the above scenario, two seconds made sense to the cardiologists we consulted. In an ultrafast arriving data stream, the permissible lag may be as little as 0.1 seconds, and for telemetry arriving from devices with a slow cycle rate, say the daily periodicity of pedestrian traffic, the permissible lag may be minutes to hours.

We suspect that many algorithms that are referred to as online in the literature, are really effectively online. The above discussion allows us to frame our contribution. Our proposed algorithm DAMP is parameterized by a single variable called *lookahead*.

- If *lookahead* is zero, DAMP is a fast *true* online algorithm.
- If *lookahead* is allowed to be arbitrarily large, DAMP is an ultrafast batch algorithm. We should not be surprised that a batch algorithm can be much faster, as it has access to all the information at once.

And now the *raison d'etre* for our digression:

- Even if *lookahead* is a small (but non-zero) number, DAMP is effectively online algorithm, yet it retains most or all the speedup of the arbitrarily large *lookahead* algorithm.

As we will show, DAMP allows for the discovery of time series discords in ultra-fast-moving streams for the first time.

### 3 DEFINITIONS AND BACKGROUND

We begin by defining the key terms used in this work. The data we work with is a *time series*.

**Definition 2:** A *time series*  $T$  is a sequence of real-valued numbers  $t_i$ :  $T = [t_1, t_2, \dots, t_n]$  where  $n$  is the length of  $T$ .

Typically, we consider only local *subsequences* of the times series.

**Definition 3:** A *subsequence*  $T_{i,m}$  of a time series  $T$  is a continuous subset of data points from  $T$  of length  $m$  starting at position  $i$ .  $T_{i,m} = [t_i, t_{i+1}, \dots, t_{i+m-1}]$ ,  $1 \leq i \leq n - m + 1$ .

The length of the subsequence is typically set by the user based on domain knowledge. For example, for most human actions,  $\frac{1}{2}$  second may be appropriate, but for classifying transient stars, three days may be appropriate.

If we take any subsequence  $T_{i,m}$  as a query, calculate its distance from all subsequences in the time series  $T$  and store the distances in an array in order, we get a *distance profile*.

**Definition 4:** *Distance profile*  $D_i$  for time series  $T$  refers to an ordered array of Euclidean distances between the query subsequence  $T_{i,m}$  and all subsequences in time series  $T$ . Formally,  $D_i = d_{i,1}, d_{i,2}, \dots, d_{i,n-m+1}$ , where  $d_{i,j}$  ( $1 \leq i, j \leq n - m + 1$ ) is the Euclidean distance between  $T_{i,m}$  and  $T_{j,m}$ .

For distance profile  $D_i$  of query  $T_{i,m}$ , the  $i^{th}$  position represents the distance between the query and itself, so the value must be 0. The values before and after position  $i$  are also close to 0, because the corresponding subsequences have overlap with query. Our algorithm neglects these matches of the query and itself, and instead focuses on *non-self match*.

**Definition 5: Non-Self Match:** Given a time series  $T$  containing a subsequence  $T_{p,m}$  of length  $m$  starting at position  $p$  and a matching subsequence  $T_{q,m}$  starting at  $q$ ,  $T_{p,m}$  is a *non-self match* to  $T_{q,m}$  with distance  $d_{p,q}$  if  $|p - q| \geq m$ .

With the definition of non-self match, we can define *time series discords*.

**Definition 6: Time Series Discord:** Given a time series  $T$ , the subsequence  $T_{d,m}$  of length  $m$  beginning at position  $d$  is said to be a discord of  $T$  if the distance between  $T_{d,m}$  and its nearest non-self match is maximum. That is,  $\forall$  subsequences  $T_{c,m}$  of  $T$ , non-self matching set  $M_D$  of  $T_{d,m}$ , and non-self matching set  $M_C$  of  $T_{c,m}$ ,  $\min(d_{d,M_D}) > \min(d_{c,M_C})$ .

Although there are many ways to locate time series discord, the most effective one recently is the *matrix profile* [39].

**Definition 7:** A *matrix profile*  $P$  of a time series  $T$  is a vector storing the z-normalized Euclidean distance between each subsequence and its nearest non-self match. Formally,  $P = [\min(D_1), \min(D_2), \dots, \min(D_{n-m+1})]$ , where  $D_i$  ( $1 \leq i \leq n - m + 1$ ) is the distance profile of query  $T_{i,m}$  in time series  $T$ . It is easy to see that the highest value of the matrix profile is the time series discord.

As we will explain below, we can compute a special matrix profile which only looks to the past. We call it the *left matrix profile*.

**Definition 8:** A *left matrix profile*  $P^L$  of a time series  $T$  is a vector that stores the z-normalized Euclidean distance between each subsequence and the nearest non-self match appearing before that subsequence. Formally, given a query subsequence  $T_{i,m}$ , let  $D_i^L = d_{i,1}, d_{i,2}, \dots, d_{i,i-m+1}$  be a special distance profile that records only the distance between the query subsequence and all subsequences that occur before the query, then we have  $P^L = [\min(D_1^L), \min(D_2^L), \dots, \min(D_{n-m+1}^L)]$ .

Note that the term discord in this paper refers to the highest value on the left matrix profile  $P^L$ , i.e., left-discord. For the sake of simplicity, we will refer to left-discord as discord where there is no ambiguity. It is clear that in the *online* case, we must use the Left-MP. However, here we argue that even in the *offline* case we should use it. To see why, consider the example shown in Fig. 5.



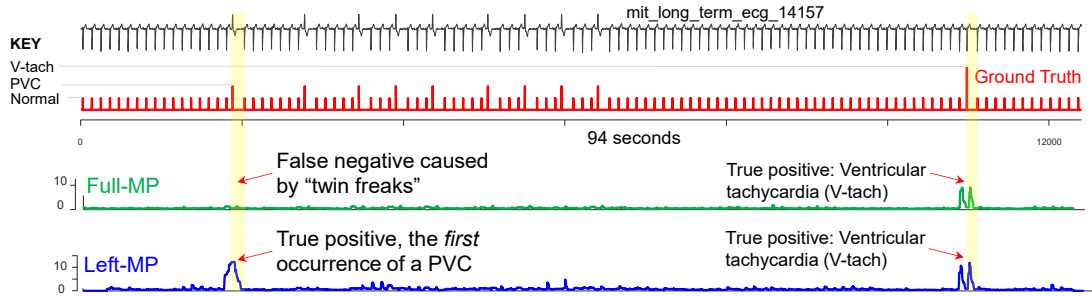


**Fig. 5** *top to bottom*) A snippet of ECG with two types of anomalous heartbeats indicated by a ground truth vector. A full Matrix Profile can find the sole occurrence of V-tach, but is confused by the multiple occurrences of PVCs (twin-freaks) and cannot find them. In contrast, the Left-MP flags the first occurrence of a PVC and the first (and only) V-tach.

Here left-discords solve the twin-freak problem by reporting the *first* occurrence of the anomaly (later occurrences, if of interest, can be trivially found with subsequence search/monitoring).

## 4 RELATED WORK

In recent years, there has been a surge of research interest in the topic of time series anomaly detection. For a detailed review, we refer the interested reader to [1][2][4][14][21][31] and the references therein. In addition to the work listed in Section 2, we have also compiled a longer annotated biography at [10] that explicitly discusses discords.

There are two important points that we have gathered from our survey of the literature. The first is due mostly to a single paper [35], that forcefully suggests some of the apparent success of recently proposed algorithms may be questionable, due to severe problems with the commonly used benchmarks in this area.

Beyond four issues that [35] notes with benchmarks datasets, we wish to add another issue. Most of these benchmarks are minuscule. We suspect that the small datasets that the community has focused on are at least partly due to the poor scalability of current approaches. For example, a recent paper examines time series of length 140,256 and notes “*Given the length of the dataset, we sub-sample it by a factor 10.*” [1]. This paper is by a research group at Amazon, who presumably does not lack for computational resources. For reference, DAMP takes 0.9 seconds of the *full*-sized version of this dataset [10] on a commodity desktop.

In addition to the problems caused by using poor quality benchmarks, a recent paper suggests yet another compelling reason why much of the recent apparent success of recent research efforts should be viewed with caution. Paper [12] notes that “*most recent approaches employ an inadequate evaluation criterion leading to an inflated F1 score. (however) a rudimentary Random Guess method can outperform state-of-the-art detectors in terms of this popular but faulty evaluation criterion.*”.

A recent SIGKDD workshop keynote makes a related point about evaluation [16]. Suppose you have a year of data monitoring an industrial boiler, and it happens that on Xmas, the boiler leaks all day, causing an anomaly. One might imagine the best way to evaluate an algorithm on the task of discovering this anomaly would be a binary score, success/failure. However, many papers essentially consider each datapoint as if it was an independent event. Suppose they predicted all of Xmas day, and the first minute of the next day was an anomaly. They would report an F1 score of 0.9997. The four significant decimal digits imply some extraordinarily careful and significant measurement was made. However, with a little introspection will allow the diligent reader to see that this precision is unwarranted and misleading. The Time Series Anomaly Detection (TSAD) literature is replete with impressively large tables of numbers with four (and sometimes, five or six!) digits, that simply give the illusion of progress and rigor.

It is somewhat surprising that so few papers in the literature discuss time complexity. This can possibly also be attributed to issues with the benchmark datasets. For example, by far the two most discussed datasets in the literature are Yahoo and NY-Taxi (NAB), with lengths of 1,200 and 10,321 respectively. Even the most sluggish of algorithms are unlikely to be taxed by such tiny datasets. If building a particular highly-quality anomaly detection algorithm had a high *one-time* cost, then we might be willing to throw whatever computational resources are needed at the task, and then deploy the model in perpetuity. However, the situation is worse than that. In virtually any domain, the model will become stale due to concept drift, and need to be periodically retrained, either on a regular schedule (say once a week), or when the model detects that it has drifted from the newly arriving data.

Recently a handful of papers have recognized that the slow training times for deep learning anomaly detectors can be an issue. For example, [32] notes that “*fast training*

*times* (are needed) *to cope with the requirement of frequently re-updating the learning model.*”. These authors then went on to introduce a “light-weight” anomaly detection system that can complete training in as little as twenty minutes (using GPUs) in a dataset of size 274,627. This kind of time frame may work for some domains, for example the three-year-long energy grid/weather data we consider in Section 6.1. We surely could afford a few hours to build the model, and perhaps a few hours at the end of each month to retrain it. However, consider the machining dataset we examine in Section 6.2. Here we see the first thirty seconds of data, and then must *instantly* have a working model. While DAMP *can* do this, it is not clear that any other anomaly detector in the literature can. One might imagine that other methods could potentially look only at say, the first twenty seconds of data, and use the remaining ten seconds to build their model. However, this would require most of the algorithms in the literature to be accelerated by several orders of magnitude.

A recent paper [26] compared twelve anomaly detection algorithms on 13,766 datasets. The datasets are a mixture of existing datasets and datasets created by the authors. There is a clear and unambiguous finding, two algorithms, the Matrix Profile and NORMA (a sort of Matrix Profile variant) are significantly better than all the other approaches. In fact, the news here is particularly good for our proposed approach. In a personal communication one of the authors [25], he revealed that many of the original datasets they made were specifically created to have the twin-freak problem (recall Fig. 5), in order to suppress the performance of the Matrix Profile. However, recall that the left matrix profile does not have an issue with twin-freaks. Consider Fig. 6. which shows three examples (of many) of the time series contrived to make the Matrix Profile underperform relative to NORMA [25]. Note that in every case, the left Matrix Profile correctly finds the anomaly.

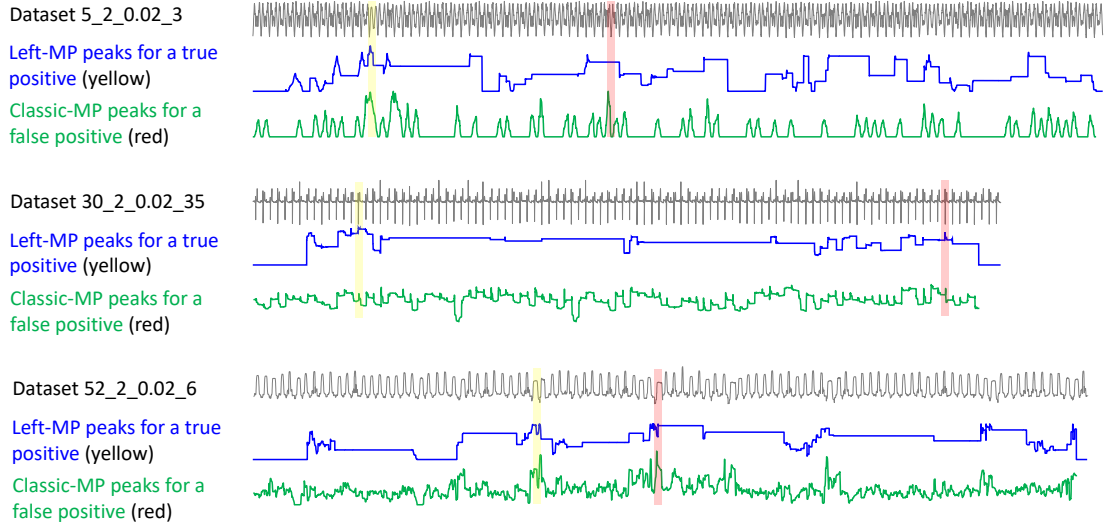


**Fig. 6** Three examples of synthetic datasets contrived by [26] to make the Matrix Profile underperform. Interestingly, there is a historical precedent for this. A 2009 paper also created a synthetic data designed to make Matrix Profile underperform [6]. What is interesting about these papers is that in both cases they were unable to find a *real* dataset that had a twin-freak problem, both resorted to creating synthetic datasets. In any case, we will show that DAMP makes this a moot point.

Finally, the reader may wonder why we do not test on the large collection of datasets in [26] in our empirical section. There are two reasons. First, the data collection includes datasets that [35] notes are deeply flawed, including mislabeled ground truth. If even a handful of datasets have mislabeled ground, as Wu and Keogh point out [35], and which the authors of [26] have acknowledged [25], it is hard to have any faith in evaluation on the overall data collection. Secondly, the agenda of creating datasets to make the Matrix Profile underperform (relative to NORMA) was not stated in the paper [26], and was only revealed [25] after we pointed out that it is obvious to anyone that examined the data. We should be wary of this dataset in case there are other unspoken agendas. In any case, testing on small synthetic unrealistic datasets seems pointless when we can test on large real datasets, as we do in this work.

## 5 DAMP

### 5.1 Intuitive Overview of DAMP

Before giving a formal explanation of our algorithm, we will first provide an intuitive description of how it works. We will start with discussing the batch case and then

further generalize to the (minor) steps required for the online case. As shown in Fig. 7, it will be helpful to explain the algorithm mid-execution, as it is processing the subsequence  $T_i$ .

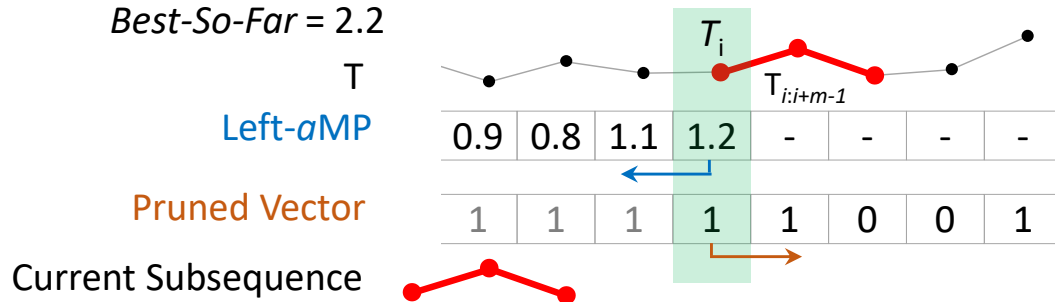


**Fig. 7** A sketch of the DAMP algorithm in progress, processing the current subsequence. *top*) The time series  $T$ . *center*) The Left- $a$ MP, its values between 1 and  $i$  are computed, its values after  $i$  have yet to be computed. *bottom*) the Pruned Vector indicates subsequences that can be ignored without affecting the final result.

Fig. 7.*top* shows the time series  $T$  being processed, the green bar indicating the current subsequence being processed at location  $i$ . Note that we have created two parallel vectors to accompany  $T$ . The Left- $a$ MP is the vector we are computing. It is an approximation to the true Left-MP, with the following properties:

- If location  $j$  is the true left-discord for the time series  $T_{1:j}$ , then the discord value at  $aMP_j$  is not an approximation, but the true left-discord value.
- Otherwise, the approximation at  $aMP_j$  is strictly bounded:  $MP_j \leq aMP_j \leq \max(MP_{1:j})$

These properties tell us that we can take any prefix of  $T$  (inducing the special case of the entire length of  $T$ ), and the left-discord reported by the Left- $a$ MP will be the same as that reported by the Left-MP.

In Fig. 7.*bottom* we show the other parallel vector that accompanies  $T$  and the Left- $a$ MP $_j$ . The Pruned Vector tells us which subsequences could not be the left-discord, and hence do not need to be processed. At initialization time, this vector is set to all ‘1’s, indicating that all subsequences must be processed. However, as we process the data, we may be able to “peek into the future” and cheaply determine locations that could not be a discord, and flip their corresponding bits to ‘0’.

At the  $i^{\text{th}}$  location, the processing can be divided into two independent steps, *backward* processing and *forward* processing.

### 5.1.1 Backward Processing

The main task of backward processing is to discover whether the current subsequence  $T_{i:i+m-l}$  is the left-discord, for which the naïve way would be to compute its nearest neighbor distance to any subsequences in  $T_{l:i}$ .

However, note that in general we may not need to find the nearest neighbor, any neighbor whose distance is less than the *Best-So-Far* will disqualify the current subsequence from being the discord. This suggests an early abandoning scheme that we can optimize with the two following observations:

- Instead of incrementally searching from the beginning, we should expect to be able to abandon earlier if we search *backwards* from the  $i^{\text{th}}$  location. The reason this is true is that the patterns can drift over time. In other words, the pattern most likely to be similar to the current subsequences is generally the subsequence *just* before the current subsequence<sup>2</sup>.
- The MASS algorithm is optimized for queries with powers of two length. For example, using the machine that performed all the experiments in this paper, we find that a MASS search with a query of length 512, takes 0.025 seconds for a time series of length 524,288 (i.e.,  $2^{19}$ ). But if we delete a single point to get a 524,287, it takes 0.177 seconds. This suggests we should attempt to construct a backward search algorithm that is comprised mostly or solely of such  $p^{\text{integer}}$  length queries.

These two observations suggest an algorithm. We should look backwards at the prefix that is the next power-of-two longer than  $m$ . If that yields a neighbor that is less than the *Best-So-Far* (*BSF*) we are done, we simply place that value in  $aMP_i$  as our approximation. If that was not the case, we double the length of the prefix to *two* times the next power-of-two longer than  $m$ , and try again. We continue to iteratively double until we find a nearest neighbor distance that is less than the *Best-So-Far*, or until our prefix includes the full span back to the beginning of  $T$ . In that latter case, we use the nearest neighbor distance to update both the *Best-So-Far* and  $aMP_i$ .

---

<sup>2</sup> This observation is true for heartbeats, gaits, machine cycles etc. One exception is for events tied to a cultural calendar. For example, for taxi demand or electrical power demand, the most similar day to any given day, is not the previous day, but the same day one week earlier.

### 5.1.2 Forward Processing

In the forward processing step, we attempt to discover and prune subsequences that cannot be left-discord. If we take the current subsequence and compare it to the suffix of  $T$ , that is, to  $T_{i+m:n}$  (the search must start at  $i+m$  to avoid self-match), any subsequence that is less than the *Best-So-Far* distance to the current subsequence can be pruned (have its corresponding bit in the Pruned Vector set to ‘0’).

In principle, we could do this search from  $i+m$  to the end. However, the two observations in the previous section still apply. While the next few cycles may be similar and yield a good pruning rate, over time the patterns tend to drift and the pruning rate falls. The combination of a long expensive similarity search and the lower pruning rate means that the forward step may not “pay” for itself. So instead, we can look forward a limited amount, say *four* times the next power-of-two longer than  $m$ .

After completing both the backward and forward processing, the algorithm increments the current pointer from  $i$  to the next index which has a ‘1’ in the Pruned Vector, and repeats the two processing steps.

### 5.2 Formal Pseudocode for DAMP

Here we give the pseudocode shown in Table 1 to formalize the intuition of the previous sections. For ease of explanation, we first consider only the batch case.

**Table 1: The Main DAMP Algorithm**

Function: DAMP( $T, m, spIndex$ )	
Input: $T$ : Time series	
$m$ : Subsequence length	
$spIndex$ : Location of split point between training and test data	
Output: aMP: Left approximate Matrix Profile	
1	$PV = \text{ones}(1, \text{length}(T) - m + 1)$
2	$aMP = \text{zeros}(1, \text{length}(T) - m + 1)$
3	$BSF = 0$ // The current best discord score
4	// Scan all subsequences in the test data
5	<b>For</b> $i = spIndex$ <b>to</b> $\text{length}(T) - m + 1$
6	<b>If NOT</b> $PV_i$ // Skip the pruned subsequence
7	$aMP_i = aMP_{i-1}$
8	<b>Else</b>
9	$[aMP_i, BSF] = \text{BackwardProcessing}(T, m, i, BSF)$
10	$PV = \text{ForwardProcessing}(T, m, i, BSF, PV)$
11	<b>return</b> aMP

In lines 1 and 2 we initialize two vectors that are essentially the same length as the time series  $T$ , but are actually of length  $n-m+1$ . These are  $PV$  (Pruned Vector), a Boolean vector that indicates which indices can be dismissed without evaluation, and  $aMP$ , which is the approximate Matrix Profile we wish to compute. The current highest discord score encountered during execution is stored in the  $BSF$ , initialized to zero in line 3.

In lines 5 to 10, we iterate through all subsequences of length  $m$  in the test data. In each iteration, we first determine whether the current subsequence was pruned, i.e., whether it is marked as 0 in the  $PV$  (line 6). If yes, we assign the discord score of the previous subsequence to the current subsequence and then skip to the next subsequence (line 7). If the current subsequence was not pruned, we must process it. In line 9 we call `BackwardProcessing` to calculate the discord score of the current subsequence. In particular, if the backward search finds a value higher than the current highest discord score ( $BSF$ ), `BackwardProcessing` returns the *exact* score of the current subsequence and updates the  $BSF$ ; otherwise, `BackwardProcessing` returns an approximate score of the current subsequence and does not update the  $BSF$ . Note that while this score is approximate, it is bounded between the true score and the current  $BSF$ .

At this point we have completely processed the current location. However, before we increment our loop index to process the next location, we take a brief digression. We will use the current subsequence to look “forward”, finding any subsequences ahead of it that have a distance to it that is less than the current  $BSF$ . It is easy to see that any such subsequences could not be a better discord than the current  $BSF$ , as when they do `BackwardProcessing`, they would find the current subsequences to be close enough to disqualify them. This observation allows us to prune these “near-enough” neighbors of the current subsequence. Concretely, line 10 invokes `ForwardProcessing` to find out the subsequences that can be pruned within a specific range in the future (if any), and their corresponding vectors are marked as 0 and recorded in the Pruned Vector  $PV$ . Finally in line 11 we return the left approximate Matrix Profile computed by the DAMP algorithm.

Table 1 provides a high-level overview of how the DAMP algorithm works. Let us now “zoom in” and look at the two core subroutines of DAMP, `BackwardProcessing` and



ForwardProcessing. We begin with Table 2 to explain backward processing, whose intuition we laid out in Section 5.1.1.

**Table 2: DAMP Backward Processing Algorithm**

Function:	$[aMP_i, BSF] = \text{BackwardProcessing}(T, m, i, BSF)$
Input:	$T$ : Time series $m$ : Subsequence length $i$ : Index of current query $BSF$ : Highest discord score so far
Output:	$aMP_i$ : Discord value at position $i$ $BSF$ : Updated highest discord score so far
1	$aMP_i = \text{inf}$
2	$prefix = 2^{\text{nextpow2}(m)}$ // Initial length of prefix
3	<b>While</b> $aMP_i \geq BSF$
4	<b>If</b> the search reaches the beginning of the time series
5	$aMP_i = \text{min}(\text{MASS}(T_{1:i}, T_{i:i+m-1}))$
6	<b>If</b> $aMP_i > BSF$ // Update the current best discord score
7	$BSF = aMP_i$
8	<b>break</b>
9	<b>Else</b>
10	$aMP_i = \text{min}(\text{MASS}(T_{i-prefix+1:i}, T_{i:i+m-1}))$
11	<b>If</b> $aMP_i < BSF$
12	<b>break</b> // Stop searching
13	<b>Else</b> // Double the length of prefix
14	$prefix = 2 * prefix$
15	<b>return</b> $aMP_i, BSF$

In line 1 we begin by initializing the discord score of the current query at position  $i$  to positive infinity. Then in line 2 we specify the initial length of the backward processing and store it in the variable  $prefix$ . We employ  $2^{\text{nextpow2}(m)}$  to define this initial length. Specifically, when we feed the subsequence length  $m$  into  $2^{\text{nextpow2}(m)}$ , it will return the smallest power of 2 greater than  $m$ . Recall that we are doing this because MASS is significantly faster when the length of the time series is a power of two. Since we are going to do a “piecewise” search of the time series that precedes the subsequence being processed, it makes sense to make these pieces be a power of two in length.

The loop in lines 3-14 evaluates the exact or approximate discord score of the current query. Here we adopt the idea of “iterative doubling”. At the beginning, we find the nearest neighbor of the current query in the initial length  $prefix$  and save the distance between the current query and the nearest neighbor into  $aMP_i$  (line 10). If this distance is lower than the current highest discord score, this means that we find a nearest

neighbor for the current query within *prefix* that is more similar than the current discord and its nearest neighbor, so it cannot be a discord, and the iteration terminates (lines 11-12). However, if the distance between the query and its nearest neighbor  $aMP_i$  is higher than the current highest discord score  $BSF$ , we double the length of the backward processing and continue the search in the next iteration (lines 13-14). This idea is visualized in Fig. 8.

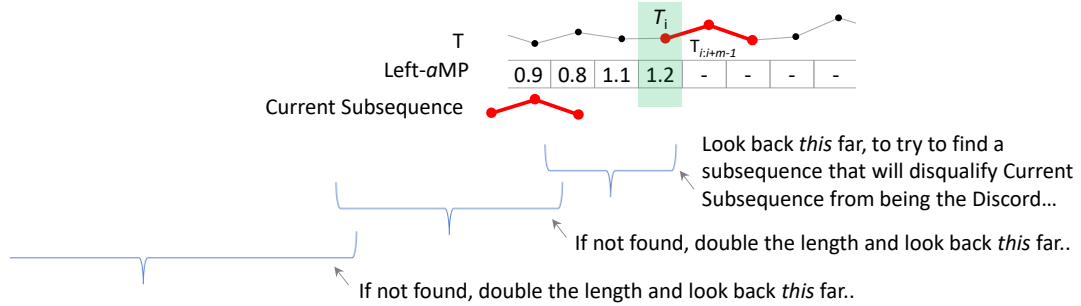


**Fig. 8** A visualization of the *iterative doubling* search policy used in lines 10-14 of Table 2. See also Fig. 7.

We keep iteratively doubling until we compute a score smaller than the  $BSF$  within the range *prefix*, or search to the beginning of the time series  $T$ . If the search gets to the beginning of the time series, we first find the nearest neighbor of the query from position 1 to  $i$  and store the distance to the nearest neighbor in  $aMP_i$  (lines 4-5). After that, we will check whether  $aMP_i$  is still larger than  $BSF$  (line 6). If yes, this means that we cannot find a nearest neighbor that is similar enough to the current query, and clearly, the current query is the new discord. In this case, we will update the highest discord score and break out of the loop (lines 7-8). Finally, line 15 returns the result of backward processing, the score of the current query  $aMP_i$ , and the current highest discord value  $BSF$ .

Note that if the search reaches the very beginning of the time series, our computation is performed in the global region (from 1 to  $i$ ), not in the local region *prefix*, in which case the discord score of the current query  $aMP_i$  is an *exact* value; whereas if our score is computed in the local region *prefix*,  $aMP_i$  is an approximate value, but bounded between the true score and the current  $BSF$ .

If we *just* use the backward processing step (line 9 of Table 1), then we have a fast online algorithm to compute the  $aMP$ . However, the use of forward processing as

outlined in Table 3 can speed up the processing by at least a further order of magnitude. This is the algorithm whose intuition was laid out in Section 5.1.2.

**Table 3: DAMP Forward Processing Algorithm**

Function:	$PV = \text{ForwardProcessing}(T, m, i, BSF, PV)$
Input:	$T$ : Time series $m$ : Subsequence length $i$ : Index of current query $BSF$ : Highest discord score so far $PV$ : Pruned Vector
Output:	$PV$ : Updated Pruned Vector
1	$lookahead = 2^{\text{nextpow2}(m)}$ // Length to "peek" ahead
2	<b>If</b> the search does not reach the end of the time series
3	$start = i + m$
4	$end = \min(start + lookahead - 1, \text{length}(T))$
5	$D'_i = \text{MASS}(T_{start:end}, T_{i:i+m-1})$ // Definition 4
6	$indices = \text{all indices in } D'_i \text{ with values less than } BSF$
7	$indices = indices + start - 1$ // Convert indices on distance
8	//profile to indices on time series
9	$PV_{indices} = 0$ // Update the Pruned Vector
10	<b>return</b> $PV$

The purpose of forward processing is admissible pruning. That is, if there is evidence that some future subsequences cannot be a discord, we will ignore these subsequences and no longer perform expensive processing on them. To achieve this in line 1 we need to define *lookahead*, the range of how many subsequences to peek ahead. Here we also use  $2^{\text{nextpow2}(m)}$ , i.e., the smallest power of 2 larger than the subsequence length  $m$ . After that, we need to determine whether the forward search exceeds the range of  $T$  to ensure that our processing is safe and there is no out-of-bounds problem (line 2). Line 3 defines the start position of the forward search, namely *start*. To avoid self-matching, we set the *start* to the position after the end of the query, that is,  $i+m$ . Line 4 explicitly defines the end position of the forward search, and since the length of our forward search is *lookahead*, or  $n$ . We can easily conclude that *end* is  $start + lookahead - 1$ . In line 5, we calculate the distance profile  $D'_i$  by calling the MASS function.

The distance profile  $D'_i$  here is slightly different from the one described in Definition 4 because it is computed under a specific range. That is,  $D'_i$  stores the distance between the current query and all subsequences in the range of *lookahead* (from *start* to *end*) instead of the distance between the current query and all subsequences of  $T$ . Once the

distance profile  $D'_i$  is constructed, we can use it for pruning. Suppose there exist subsequences in the future that are more similar to the current query than the discord to its nearest neighbor. In that case, these subsequences cannot be a discord, so we can prune them. Therefore, we can use the current highest discord score  $BSF$  as a criterion to find all the indices in the distance profile with values lower than the  $BSF$  (line 6). Since the indices on the distance profile start at 1 and are not aligned with the true indices of the time series, we need an additional step in line 7 to convert the indices on the distance profile to the true indices of the subsequence. After line 7 we get a list of indices for the subsequences that can be pruned out. The Pruned Vector values at the corresponding positions specified in the list *indices* are set to 0 (line 9), indicating that when later iterations process the subsequences listed in *indices* we can simply skip them. At last, line 10 returns the updated Pruned Vector  $PV$ .

The forward processing algorithm has exactly one parameter, the *lookahead* length. How should we set this? In Fig. 9.*left* we sketch out the tradeoffs involved. A longer *lookahead* can prune more subsequences, but this comes at the cost of more expensive similarity searches. The good news is that the speedup is dramatic, that the sweet spot is early (given us effectively online detection), and that the exact value of the *lookahead* parameter is not too critical. All datasets we examined exhibit this “U-shaped” behavior, although the similarity searches. As Fig. 9.*right* shows, this intuition is borne out by experiment. The height of the base of the “U” can be lower (smooth and highly periodic data) or higher.

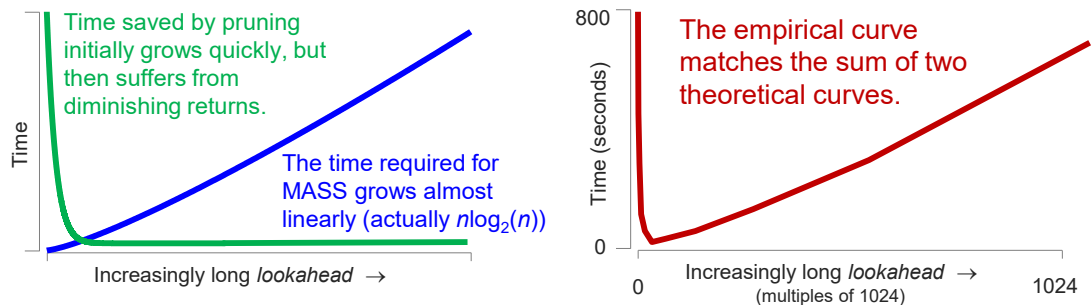


**Fig. 9** *left*) The *lookahead* tradeoff is based on two factors. As the *lookahead* grows, the pruning rate becomes greater, but the cost of the similarity search increases. *right*) The empirically measured effectiveness of forward processing (on random walks of length  $2^{20}$ ) is indeed the sum of the two factors.

Finally, this is a good place to mention an important caveat about interpreting a Left-AMP that is computed using forward processing. Failure to understand this caveat may

lead a user to think the  $aMP$  is indicating an anomaly where there is none. Consider Fig. 10 which shows DAMP processing an excerpt of the MGAB, both with and without forward processing.

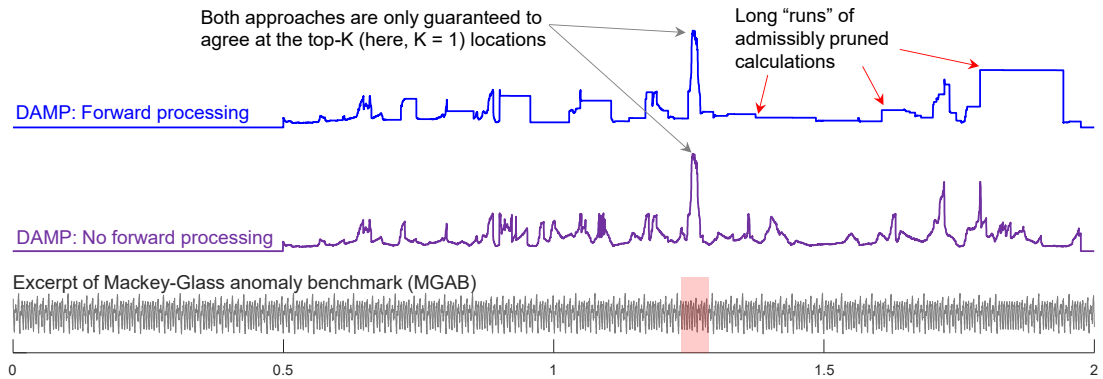


**Fig. 10** *bottom-to-top*) An excerpt of the MGAB with an anomaly highlighted in red. The top-1 Left- $aMP$  computed without using forward processing. The top-1 Left- $aMP$  computed without forward processing produces long constant runs that indicate that the algorithm admissibly skipped those regions.

When using DAMP with forward processing to search for the top- $k$  left-discords, the  $k$  highest peaks *do* correctly show the location and strength (the height of the peaks) of the top- $k$  left-discords (in Fig. 10,  $k = 1$ ). However, the remaining  $k + 1$  peaks should not be assumed to indicate slightly smaller anomalies. They simply indicate regions that were pruned by encountering a matching subsequence that was below the current *Best-So-Far*. For example, towards the end of the forward processing variant of DAMP in Fig. 10 there is a long constant plateau with a relatively high value. As we can see by comparing that region to the no-forward-processing region just below it, we should not assume that there are any anomalies in that region.

Again, to summarize: The top- $k$  peaks of the top- $k$  Left- $aMP$  do indicate the correct values of top- $k$  discords of  $T$ , but the remaining values of the top- $k$  Left- $aMP$  have no direct interpretation.

### 5.2.1 The Time and Space Complexity of DAMP

Since all computation results are stored in a one-dimensional vector of size  $n$ , the space complexity of DAMP is just the size of the original data,  $O(n)$ . The worst-case time complexity is  $O(n \log n)$  per datapoint ingested, the time required to do a full similarity search with MASS [19]. However, empirically, on diverse real-world datasets, more than 99.999% of the times we enter the loop in line 3 of Table 2 we will break out in

the first iteration (line 12), making the algorithm effectively  $O(m \log m)$  per datapoint ingested, and linear in the time series length. Fig. 24 shows this linear assumption strongly holds up to at least  $n = 2^{30}$ .

### 5.3 DAMP Variants

There are more general cases that can be easily handled by modifying the basic DAMP, for example:

- The algorithm as explained in Table 1 is a *batch* algorithm. To make it an *online* algorithm, we simply must reduce the size of the *lookahead* (Table 3, line 1) to the largest delay we are willing to accept (including possibly *zero* delay).
- The algorithm as explained in Table 1 computes the Left-*a*MP, however we can modify it to compute the classic Full-*a*MP. If the backward processing step reaches the beginning of the time series, instead of updating the *BSF*, we do the same type of iterative doubling search, but *forward* from the current index (not to be confused with forward pruning search in Table 3). We have made this code available at [10], but we do not consider it further here, due to page limits.
- It may be useful to limit how far back the backward processing can look, essentially redefining anomalies as “*the subsequence with the maximum distance to any of the X subsequences before it*”. We call this variant the *X-Lag-Amnesic DAMP*.
- Instead of searching an ever-growing amount of previously seen data in the BackwardProcessing step, we can search a fixed pool of explicit training data. For example, an engineer could curate a dataset that contains all the allowable behaviors for a manufacturing process (i.e., the “*Golden Batch*”).

There are several other useful variants that we have considered, and we suspect the community will quickly exploit the scalability of the basic DAMP algorithm to invent further variants.

Below we give more details about the two useful variants of DAMP, *X-Lag-Amnesic DAMP* and *Golden DAMP* mentioned above. To help the reader better understand how these two variants work, let us start with the most basic variant, namely, *Classic DAMP*.

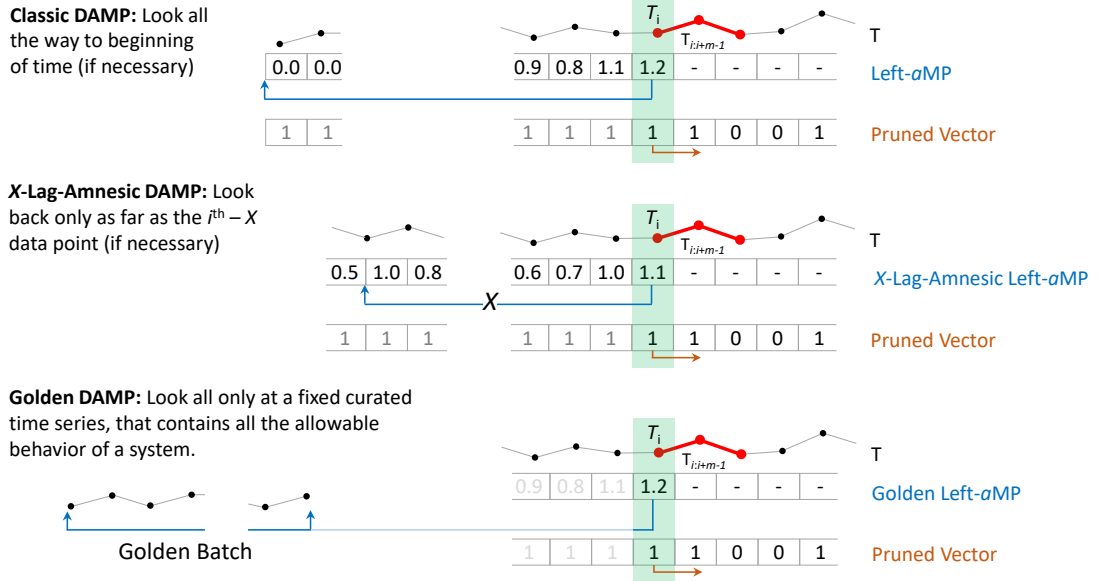


**Fig. 11** Three variants of DAMP. *top*) Classic DAMP *middle*) X-Lag Amnesic DAMP *bottom*) Golden DAMP

The Classic DAMP algorithm illustrated in Fig. 11.*top* was already discussed in Sections 5.1 and 5.2. It is worth noting here that for Classic DAMP, all data collected before the current time  $T_{1:i-1}$  are our training data by default, and our backward search is executed on this progressively growing training data. This means that to calculate the discord score of the current subsequence  $T_{i:i+m-1}$ , Classic DAMP searches all the way forward from position  $i$  by the iterative doubling process, and, in the worst case, all the way to the beginning of the time series, i.e.,  $T_{1:i}$ . Therefore, as we process more and more data points over time, our backward search may also require more and more time. As we shall see in our experimental section, empirically this is not a problem on the dozens of datasets we consider. Nevertheless, X-Lag-Amnesic DAMP and Golden DAMP allow us to provide a strict bound on the worst-case behavior, in addition to possessing other useful properties.

### 5.3.1 X-Lag-Amnesic DAMP

In some settings we may require an algorithm that show us the most unusual behavior in *just* the last few minutes, days, months, or years. In that case, a DAMP variant that constrains how far back the backward search can look is required. Formally, we refer to such a DAMP variant as *X-Lag-Amnesic DAMP*.

Compared with Classic DAMP, the time overhead of X-Lag-Amnesic DAMP is bounded and controllable. This is because it only cares about what happened in a fixed

unit of time before the present, and its calculation is based on fixed-size and real-time updated training data. For example, if we only need to find anomalies that occurred in the most recent month,  $X$ -Lag-Amnesic DAMP will perform an iterative doubling search in the most recent month's data rather than searching through all past data. Consequently, the time cost of  $X$ -Lag-Amnesic DAMP is bounded by the length of  $X$  as opposed to increasing gradually.

In addition,  $X$ -Lag-Amnesic DAMP can better deal with concept drift. For time series in some domains, their patterns change over time and the dependence between their data weakens as the distance increases, at which point it makes no sense to consider data that is too far from the present. For example, for many batch processes in the food and beverage industry the time series patterns are known to drift over each day, due to changes in ambient temperature and humidity. A pattern that happens during the nightshift may be anomalous because the process is "running hot". It might be obvious if we compare only to the patterns in the previous hour or so, but it will not be obvious if we allow comparisons back to the previous midday. Obviously, since  $X$ -Lag-Amnesic DAMP focuses only on what happened recently, it can avoid such issues caused by concept drift. By contrast, Classic DAMP is more vulnerable to this, as its backward search may cover all data that occurred before the present, and all these data have the same weight for the discord score calculation regardless of their proximity to the current subsequence.

Fig. 11.*middle* describes how the  $X$ -Lag-Amnesic DAMP works. Here we introduce a new parameter  $X$ , the maximum length that the backward processing algorithm can look back, specified by the user as needed. The framework of the  $X$ -Lag-Amnesic DAMP algorithm is the same as Classic DAMP; it retains the forward and backward processing steps, in which the forward processing is identical to Classic DAMP. The only difference between  $X$ -Lag-Amnesic DAMP and Classic DAMP is that for the current subsequence being processed  $T_{i:i+m-1}$ , we only perform a backward search on the  $X$  data points before it, not on all the previous data. However, the search is still iteratively doubled: it terminates either when it finds the nearest neighbor with a distance smaller than the  $BSF$  or when it reaches the beginning of  $X$ . Therefore, to make  $X$ -Lag-Amnesic DAMP work, we simply need to change lines 4-5 of Table 2 for Classic DAMP to the five lines shown in Table 4.



**Table 4: Pseudo code snippet for X-Lag-Amnesic DAMP**

1	<b>If</b> Starting position of the search $< \max(i-X, 1)$ <b>Or</b> $X < prefix$
2	<b>If</b> $i - X < 1$
3	$aMP_i = \min(\text{MASS}(T_{1:i}, T_{i:i+m-1}))$
4	<b>Else</b>
5	$aMP_i = \min(\text{MASS}(T_{i-X:i}, T_{i:i+m-1}))$

In line 1 we added two new criteria for search termination, i.e., reaching the beginning of the time series  $T_{i-X:i}$ , or the maximum length of looking back  $X$  is less than the initial length of the iterative doubling search *prefix*. In both cases, we do not iteratively double our search anymore. Instead, we only search for the nearest neighbor of the current subsequence in the range  $i-X$  to  $i$  (lines 4-5). Moreover, there is a special case where the number of data points that arrived has not yet reached  $X$  ( $i < X+1$ ). In this case, we can only conduct the backward search in all available data  $T_{1:i}$  as shown in lines 2-3.

Others works have noted the utility of amnesic anomaly detection (although not using that phrase), including the SAND algorithm of [5]. However, SAND requires significant effort to build a reference dataset, and the setting of several unintuitive parameters.

### 5.3.2 Golden DAMP

Recall that Classic DAMP has a parameter called *spIndex*, which sets the location of the split point between the training and test data in the initial state. When Classic DAMP processes a time series, it assumes that the data before *spIndex*,  $T_{1:spIndex-1}$  are normal, which may lead to three issues. First, this causes the algorithm to ignore the potential anomalous behavior present in  $T_{1:spIndex-1}$ , resulting in certain false-negative results. Second, this approach may have the algorithm wasting time searching redundant data. It is possible that the patterns in  $T_{1:spIndex-1}$  are highly redundant, such as 1,000 heartbeats that are essentially identical. If the heartbeats all have the same pattern, it would suffice for the algorithm to take just one of them to learn<sup>3</sup>; there is no need to consider the same pattern 1,000 times, which will waste a lot of time. Further, it may be difficult for  $T_{1:spIndex-1}$  to contain every normal pattern, which can cause the algorithm to incorrectly identify normal behavior that does not appear in

<sup>3</sup> Actually, using exactly one heartbeat (or *pattern* more generally), may make the downstream algorithms brittle to the choice of the starting point of the heartbeat. To bypass this issue, we always extract two consecutive beats.

$T_{1:spIndex-1}$  as an anomaly. For example, if  $T_{1:spIndex-1}$  only contains data on the solar zenith angle during the day, the algorithm may incorrectly identify normal solar zenith angles at night as anomalies. These potential problems can undermine the accuracy and efficiency of the algorithm.

*Golden DAMP* is our proposed solution to the above three problems. It processes each subsequence not by referring to information that occurred before the current time, but to user-defined, curated, out-of-band information, denoted as *Golden Batch*. The Golden Batch implicitly defines every possible legal behavior, such as every possible dance move, every normal heartbeat, etc. It includes all the things the user expects to happen in the system. With this correct and comprehensive priori knowledge, the algorithm will be able to make more accurate and efficient decisions.

This idea of creating a curated collection of data that spans the space of all possible acceptable behaviors is well known in the process industry [37]. For example, food/beverage engineers will often set aside one day to create a recipe under all combinations of conditions encountered: under cool conditions, under hot conditions, with carbonated infeed, with flat infeed etc. However, the use of these batch profiles is typically human comparison of the evolving process to the Golden Batch(es) [37]. Here we are interested in automatic anomaly detection. In addition, note that while the Golden Batch data can be hand curated, it can also be created automatically by various numerosity reduction algorithms [15][36].

Further note that the execution time of Golden DAMP is also bounded because its training data is the Golden Batch with a fixed size. Therefore, as we explained in Section 5.3.1, the cost of Golden DAMP's backward search is proportional to the size of Golden Batch.

Fig. 11.*bottom* illustrates the idea of Golden DAMP. When processing the current subsequence  $T_{i:i-m+1}$ , Golden DAMP no longer looks backward in the time series  $T$  but toward the Golden Batch, a vector containing all acceptable patterns. We still use the iterative doubling search policy shown in Fig. 8 for Golden Batch. The search keeps iteratively doubling until it finds the nearest neighbor within the *prefix* whose distance from  $T_{i:i-m+1}$  is less than the *BSF*, or it gets to the beginning of the Golden Batch. After computing the approximate or exact discord score for position  $i$ , we invoke the same

forward processing procedure as in Classic DAMP to disqualify future subsequences that are unlikely to become a discord.

The implementation details of Golden DAMP are given in Table 5 and Table 6. Since most of them are the same as Table 1 and Table 2, we will highlight the parts that we changed.

**Table 5: The Main Golden DAMP Algorithm**

Function: Golden_DAMP( $T, m, GoldenBatch$ )	
Input: $T$ : Time series	
$m$ : Subsequence length	
$GoldenBatch$ : A long time series with all possible normal patterns	
Output: aMP: Left approximate Matrix Profile	
1	$PV = \text{ones}(1, \text{length}(T) - m + 1)$
2	$aMP = \text{zeros}(1, \text{length}(T) - m + 1)$
3	$BSF = 0$ // The current best discord score
4	// Scan all subsequences in the test data
5	<b>For</b> $i = 1$ <b>to</b> $\text{length}(T) - m + 1$
6	<b>If NOT</b> $PV_i$ // Skip the pruned subsequence
7	$aMP_i = aMP_{i-1}$
8	<b>Else</b>
9	$[aMP_i, BSF] = \text{BackwardProcessing}(T, m, i, BSF, GoldenBatch)$
10	$PV = \text{ForwardProcessing}(T, m, i, BSF, PV)$
11	<b>return</b> aMP

The main framework of Golden DAMP is shown in Table 5. Golden DAMP has a new input, *GoldenBatch*, a long vector that joins all normal patterns together. As with Table 1, the algorithm starts with initialization in lines 1-3. Since we already have the training data *GoldenBatch*, we no longer need to use the first  $spIndex-1$  data of the time series  $T$ . As a result, in line 5 we adjust the processing range of Golden DAMP from  $T_{spIndex:n-m+1}$  to  $T_{1:n-m+1}$ . After that, within the loop, lines 6-7 decide whether to process the current subsequence  $T_{i:i-m+1}$  according to the value in the pruned vector  $PV$ . If the subsequence at position  $i$  needs to be processed, we first invoke *BackwardProcessing* in line 9 to calculate the discord score for position  $i$  and update the current highest discord value, and then call *ForwardProcessing* in line 10 to determine the subsequences to be pruned in the future. Finally, lines 5-10 iterate through each subsequence in  $T_{1:n-m+1}$  and line 11 returns the Golden Left-aMP. In particular, the *ForwardProcessing* here is identical to that of Classic DAMP, so we do not repeat it below. However, we partially changed

*BackwardProcessing* from Table 2 of Classic DAMP, so we give Table 6 detailing the backward processing for Golden DAMP.

**Table 6: Golden DAMP Backward Processing Algorithm**

Function:	$[aMP_i, BSF] = \text{BackwardProcessing}(T, m, i, BSF, \text{GoldenBatch})$
Input:	<p><math>T</math>: Time series</p> <p><math>m</math>: Subsequence length</p> <p><math>i</math>: Index of current query</p> <p><math>BSF</math>: Highest discord score so far</p> <p><math>\text{GoldenBatch}</math>: A long time series with all possible normal patterns</p>
Output:	<p><math>aMP_i</math>: Discord value at position <math>i</math></p> <p><math>BSF</math>: Updated highest discord score so far</p>
1	$aMP_i = \text{inf}$
2	$\text{prefix} = \min(2^{\text{nextpow2}(m)}, \text{length}(\text{GoldenBatch}))$
3	<b>While</b> $aMP_i \geq BSF$
4	<b>If</b> the search reaches the beginning of the Golden Batch
5	$aMP_i = \min(\text{MASS}(\text{GoldenBatch}_{1:\text{end}}, T_{i:i+m-1}))$
6	<b>If</b> $aMP_i > BSF$ // Update the current best discord score
7	$BSF = aMP_i$
8	<b>break</b>
9	<b>Else</b>
10	$aMP_i = \min(\text{MASS}(\text{GoldenBatch}_{\text{end}-\text{prefix}+1:\text{end}}, T_{i:i+m-1}))$
11	<b>If</b> $aMP_i < BSF$
12	<b>break</b> // Stop searching
13	<b>Else</b> // Double the length of prefix
14	$\text{prefix} = 2 * \text{prefix}$
15	<b>return</b> $aMP_i, BSF$

Table 6 illustrates the backward processing algorithm of Golden DAMP. As the backward search is performed on top of Golden Batch, we need to enter *GoldenBatch* into the algorithm. The first two lines of Table 6 are still the initialization phase. Line 1 is the same as in Table 2, initializing the discord score of the current subsequence to positive infinity. In line 2 we define the initial length of the iterative doubling search *prefix*. Here we set it as the lower bound of  $2^{\text{nextpow2}(m)}$  and Golden Batch size to prevent possible array out-of-bounds problem at line 10. Then in the loop in lines 3-14, we perform the iterative doubling search, which starts from the end of Golden Batch and goes backwards. We keep searching in  $\text{GoldenBatch}_{\text{end}-\text{prefix}+1:\text{end}}$  until we find the nearest neighbor whose distance from the current subsequence is less than *BSF* (line 11) or reach the beginning of Golden Batch (line 4). Specifically, if we find the nearest neighbor within the range *prefix*, we assign the approximate discord score of the current

subsequence to  $aMP_i$  and stop the search (lines 10-12); if not, in lines 13 and 14 we double the length of  $prefix$  and continue the search in  $GoldenBatch_{end-prefix+1:end}$ . If the search finally reaches the beginning of Golden Batch (line 4), we first calculate the exact discord score of the current subsequence using all the data in  $GoldenBatch$  (line 5), and then determine whether the current highest discord score  $BSF$  needs to be updated (line 6). If the discord score of the current subsequence is still greater than  $BSF$ , it means that the subsequence at position  $i$  does not have a nearest neighbor similar enough to it in the Golden Batch and it is a discord, at which point we should update the current highest discord score  $BSF$  in line 7.

#### 5.4 Multidimensional DAMP

The previous sections have shown how to find anomalies in a one-dimensional time series. We believe that in many cases, anomaly detection of *all* the one-dimensional data is sufficient for user demands. For example, in a hospital setting, a doctor may monitor a patient's ECG, blood pressure, and respiration. Most life-threatening situations will show up in at least one of the above. For example, a myocardial infarction, will first show up in the patient's ECG, septicemia will first show up in the patient's blood pressure, and tracheomalacia will first show up in the patient's blood respiration.

However, there are also special cases where anomalies occur in only two or more dimensions. For example, in the low-latitude Pacific West Coast region, typhoons accompanied by heavy precipitation occasionally make landfall in summer. In order to identify such unusual weather events, it is insufficient to monitor *only* precipitation or wind speed. This is because these areas may have strong winds but sunny weather, or extreme rainfall but still air. As a result, we need to combine wind speed and precipitation as two-dimensional data to find out which day has both precipitation and wind speed anomalies. If such anomalies can be identified in two dimensions, there is a high chance of typhoon weather on that day. Therefore, it is necessary to generalize our DAMP algorithm to support searching in high-dimensional spaces. We refer to the DAMP algorithm for multidimensional data anomaly detection as *multidimensional DAMP*.

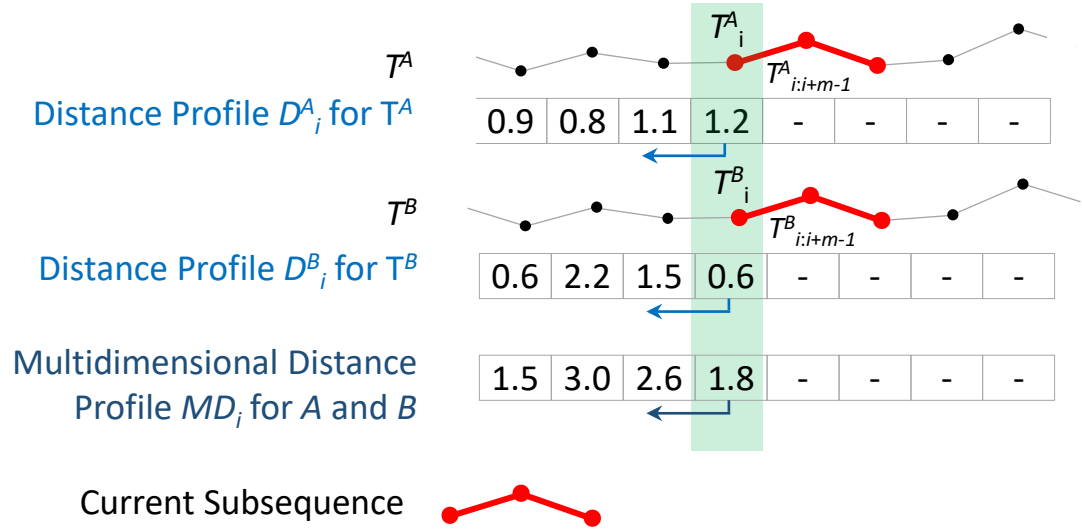


**Fig. 12** Multidimensional distance profile for position  $i$ .

The basic idea of multidimensional DAMP is the same as the one-dimensional DAMP we introduced in Section 5.1, which retains the procedure of backward iterative doubling and forward pruning. The difference between them is reflected solely in the calculation of the discord score. Fig. 12 illustrates how the multidimensional DAMP calculates the discord score for position  $i$ . Let  $T^A$  be the time series of dimension  $A$  in a two-dimensional time series, while  $T^B$  corresponds to dimension  $B$ , and the length and frequency of  $T^A$  and  $T^B$  are equal. For position  $i$ , we first compute the distances between the current subsequence of  $T^A$  and  $T^B$  and the subsequences before position  $i$  in their respective dimensions, forming two distance vectors  $D^A_i$  and  $D^B_i$  (see Definition 4). After that, we add the elements of the two distance vectors two by two according to their positions to produce a new vector  $MD_i$ , which contains the distance information in both dimensions  $A$  and  $B$ . Finally, the minimum value on  $MD_i$  is the discord score at position  $i$ . As the algorithm progresses, the  $BSF$  continuously tracks the current highest discord score that combines information from both dimensions.

Table 7 and Table 8 give the implementation details of multidimensional DAMP. Here we only demonstrate the two-dimensional version, however the reader can easily modify it to work with higher dimensional data. Since the basic steps of multidimensional DAMP and one-dimensional DAMP are the same, the framework of multidimensional DAMP is identical to Table 1.

**Table 7: Multidimensional DAMP Backward Processing Algorithm**

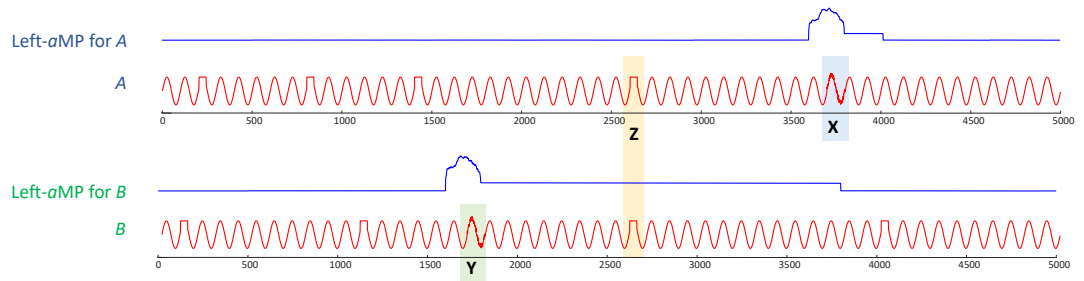
Function:	$[aMP_i, BSF] = \text{BackwardProcessing}(T^A, T^B, m, i, BSF)$
Input:	$T^A$ : Dimension A of the multidimensional time series $T^B$ : Dimension B of the multidimensional time series $m$ : Subsequence length $i$ : Index of current query $BSF$ : Highest discord score so far
Output:	$aMP_i$ : Discord value at position $i$ $BSF$ : Updated highest discord score so far
1	$aMP_i = \text{inf}$
2	$prefix = 2^{\text{nextpow2}(m)}$ // Initial length of prefix
3	<b>While</b> $aMP_i \geq BSF$
4	<b>If</b> the search reaches the beginning of the time series
5	$aMP_i = \min(\text{MASS}(T^A_{i:i}, T^A_{i:i+m-1}) + \text{MASS}(T^B_{i:i}, T^B_{i:i+m-1}))$
6	<b>If</b> $aMP_i > BSF$ // Update the current best discord score
7	$BSF = aMP_i$
8	<b>break</b>
9	<b>Else</b>
10	$aMP_i = \min(\text{MASS}(T^A_{i-prefix+1:i}, T^A_{i:i+m-1}) + \text{MASS}(T^B_{i-prefix+1:i}, T^B_{i:i+m-1}))$
11	<b>If</b> $aMP_i < BSF$
12	<b>break</b> // Stop searching
13	<b>Else</b> // Double the length of prefix
14	$prefix = 2 * prefix$
15	<b>return</b> $aMP_i, BSF$

Table 7 presents the multidimensional backward processing algorithm. As it is primarily similar to Table 2, we refer the reader to Section 5.2 for more details on the iterative doubling backward algorithm. Here we only highlight the parts that have changed. Compared to Table 2, we add two new inputs  $T^A$  and  $T^B$ , the time series in dimensions  $A$  and  $B$ . In lines 5 and 10, we change the calculation of the discord score at position  $i$   $aMP_i$ . In line 5, to obtain  $aMP_i$ , we call MASS twice to calculate the distance between the current subsequence of  $T^A$  and  $T^B$  and all subsequences before position  $i$  respectively. Next, we add the elements in the two distance vectors returned by MASS two by two according to the positions to obtain the multidimensional distance profile. Finally, the minimum value of the multidimensional distance vector is taken as the exact discord score of position  $i$ . Line 10 is similar to line 5. The only difference is that line 10 only finds the nearest neighbor in the prefixes of  $T^A$  and  $T^B$  before position  $i$  and  $aMP_i$  is the approximate discord score for position  $i$ .

**Table 8: Multidimensional DAMP Forward Processing Algorithm**

Function:	$PV = \text{ForwardProcessing}(T^A, T^B, m, i, BSF, PV)$
Input:	$T^A$ : Dimension A of the multidimensional time series $T^B$ : Dimension B of the multidimensional time series $m$ : Subsequence length $i$ : Index of current query $BSF$ : Highest discord score so far $PV$ : Pruned Vector
Output:	$PV$ : Updated Pruned Vector
1	<code>lookahead = 2^nextpow2(m) // Length to peek ahead</code>
2	<code>If the search does not reach the end of the time series</code>
3	<code>start = i + m</code>
4	<code>end = min(start + lookahead - 1, length(T))</code>
5	<code>MD'_i = MASS(T^A_start:end, T^A_i:i+m-1) + MASS(T^B_start:end, T^B_i:i+m-1)</code>
6	<code>indices = all indices in MD'_i with values less than BSF</code>
7	<code>indices = indices + start - 1 // Convert indices on distance</code>
8	<code>profile to indices on time series</code>
9	<code>PV_indices = 0 // Update the Pruned Vector</code>
10	<code>return PV</code>

Multidimensional DAMP also has a similar forward pruning process to that of one-dimensional DAMP, as shown in Table 8. Compared with Table 3, we need to only change line 5. In the range of *lookahead*, the distances between the current and future subsequences of  $T^A$  and  $T^B$  are calculated separately. Then the distance vectors of  $A$  and  $B$  dimensions are summed to yield a distance vector  $MD'_i$  containing two-dimensional information. Our pruning decisions are made based on this two-dimensional distance vector.



**Fig. 13** Synthetic time series  $A$  and  $B$ . *top*) Synthetic dataset  $A$  and its corresponding one-dimensional Left-aMP. *bottom*) Synthetic dataset  $B$  and its corresponding one-dimensional Left-aMP.

Let us start with a toy data set to understand the difference between multidimensional DAMP and one-dimensional DAMP. The red curves in Fig. 13 illustrate two synthetic time series  $A$  and  $B$ . These two time series consist mainly of sine waves. Specifically, for time series  $A$ , the data at positions 3700-3799 (**X**) are noisier than the other parts,



while for time series  $B$ , the data at positions 1700-1799 ( $Y$ ) are noisier. If you look closely, you will find that the two time series will have a square wave at random positions from time to time. It so happens that at positions 2605-2644, both time series show a square wave simultaneously, which is where our real anomaly lies. We denote it as  $Z$ . We tested the time series  $A$  and  $B$  with one-dimensional DAMP and two-dimensional DAMP respectively to see if they could find the true anomaly  $Z$ . Fig. 13 also gives the results of performing a one-dimensional DAMP on time series  $A$  and  $B$ . It is easy to see by the highest point of the blue curve in Fig. 13.*top* that one-dimensional DAMP is attracted to the noisy sine wave in  $A$  and does not notice the anomaly at position  $Z$ . Similarly, as illustrated in Fig. 13.*bottom*, one-dimensional DAMP on  $B$  also fails to detect the anomaly at  $Z$ , instead considers the noisier  $Y$  as the anomaly. Missing information in another dimension, the one-dimensional DAMPs mistakenly believe that the presence of the square wave at  $Z$  is justified because they observe similar patterns before  $Z$ .

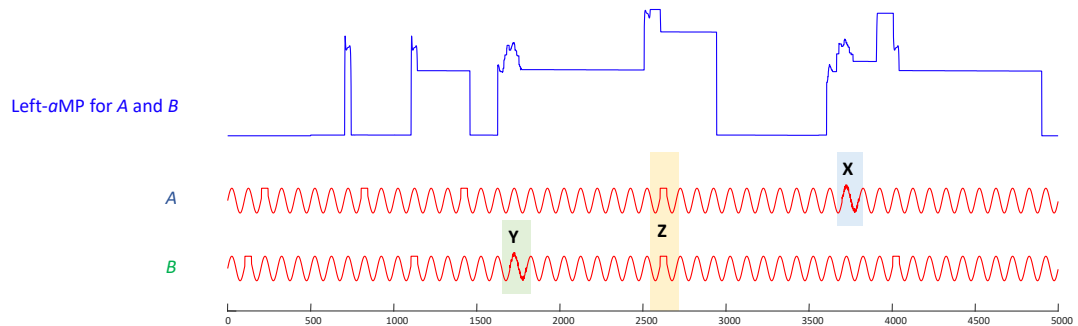
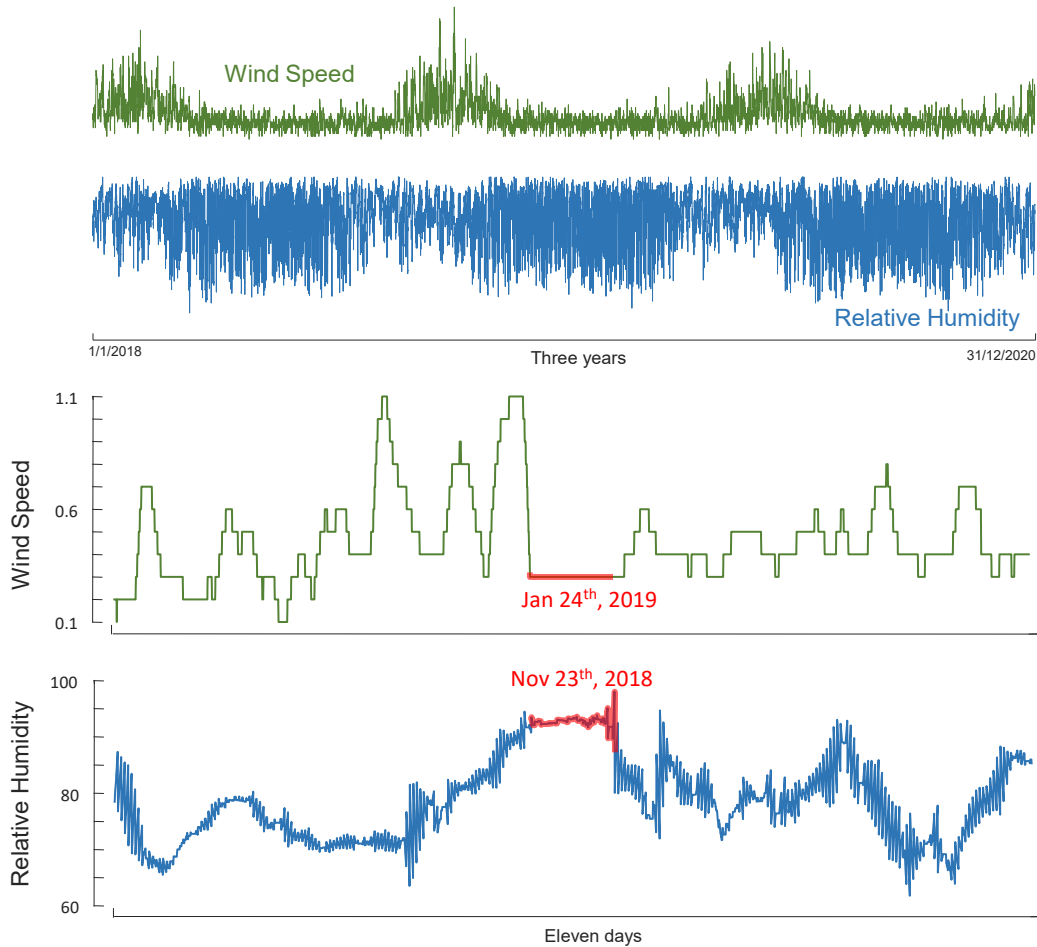


**Fig. 14** Left- $a$ MP generated by two-dimensional DAMP.

Next, we combine  $A$  and  $B$  into a two-dimensional time series and feed it into the two-dimensional DAMP to see if the results will be different. The Left- $a$ MP generated by two-dimensional DAMP is shown in Fig. 14. Note that compared with the Left- $a$ MP generated by the one-dimensional DAMP in Fig. 14, the two-dimensional Left- $a$ MP captures more anomalies with more “bumps” on its curve. All these bumps can be interpreted intuitively. For example, when both square and sine waves are present, or when one of the sine waves is noisier, they are recognized by the algorithm as a potential anomaly and correspond to a bump in the Left- $a$ MP. What is more, the position of the highest point of Left- $a$ MP in Fig. 14 corresponds to the coincidence of two square waves, that is,  $Z$ . This is because if you look at the entire time series of  $A$

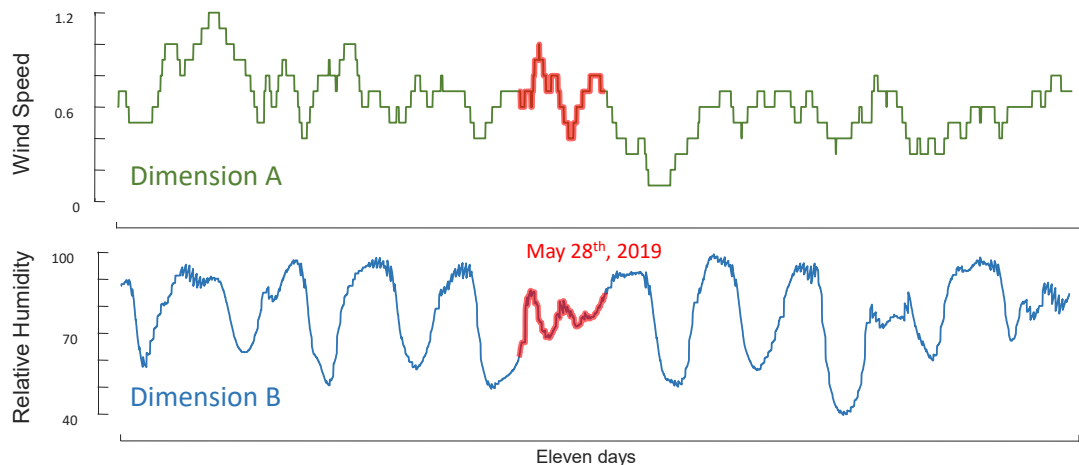
and  $B$ , you will see that the square wave only appears at  $\mathbf{Z}$  in both dimensions simultaneously, which cannot be observed at other locations.

We have seen that we can create a synthetic dataset that has an anomaly that can be discovered only by considering two time series simultaneously. However, can we discover two-dimensional anomalies in real data? Surprisingly, we are not aware of any such benchmark dataset. Most datasets in the space are synthetic, or are multidimensional, but have anomalies that are so obvious that it suffices to examine any *single* dimension [2][14]. However, we can explore energy grid data published by a consortium of Texas A&M and USC in 2021 [38], and use out-of-band data to evaluate the returned anomalies. Fig. 15.*top* shows three years of wind speed and relative humidity data from the New York area between 2018 to 2020 [38].



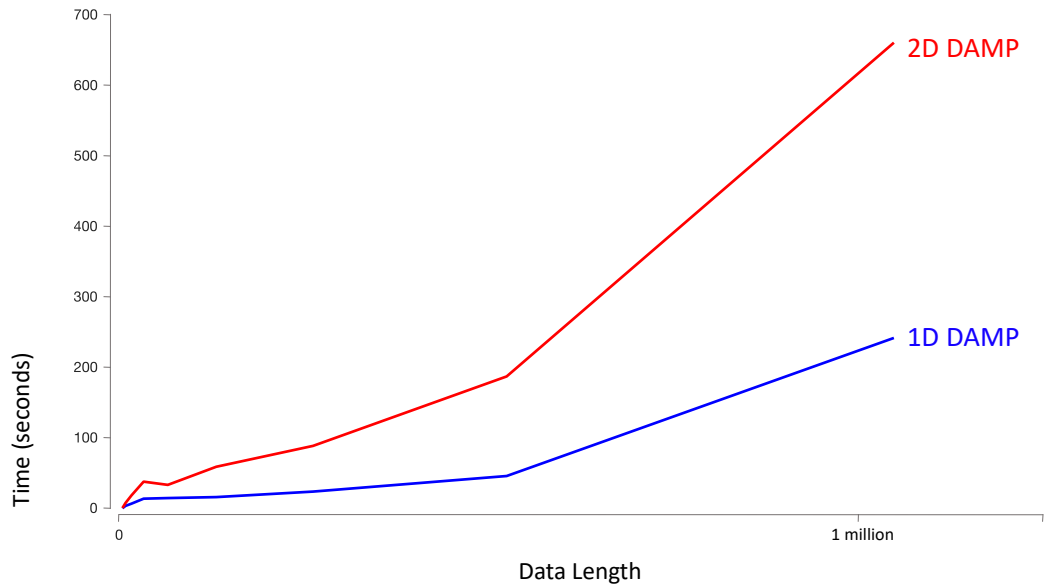
**Fig. 15** *top*) Three years of wind speed and relative humidity data for the New York area from [38]. *bottom*) The two corresponding top 2D discord in this dataset.

Fig. 15.*bottom* shows the results of our search on the one-dimensional data of wind speed and relative humidity, respectively, and the anomalies identified by one-dimensional DAMP are marked in red. First, for wind speed, the one-dimensional DAMP reports the constant interval occurring on January 24, 2019, as an anomaly; however, we do not find any reported climate anomaly in New York State on that date. That is to say, although the algorithm finds an anomaly with a pattern that is different from its context, it does not seem to noticeably affect people’s lives. As a result, we can conclude that the wind speed anomaly is trivial. Second, for relative humidity, the one-dimensional DAMP identifies the continuous peak occurring on November 23, 2018, as an anomaly. Through a Google search, we found reports of heavy rainfall and flooding that occurred in New York State on that day [22], which confirms that the anomalies identified in the dimension of relative humidity are informative and that the one-dimensional DAMP is effective.



**Fig. 16** Top discord for two-dimensional DAMP.

However, if we combine wind speed and humidity and search in two dimensions, will the algorithm give us more interesting results? To investigate this, we took wind speed as dimension A and relative humidity as dimension B and re-executed this two-dimensional data using multidimensional DAMP. The results are presented in Fig. 16. Note that the two-dimensional DAMP reports a different date to either of the one-dimensional DAMP runs, May 28, 2019. This means that *both* humidity and wind speed in New York City showed anomalous patterns on this date. This anomaly is confirmed by the news “*A powerful thunderstorm slammed Staten Island Tuesday night, pounding the borough with large hail, heavy rain and the threat of a tornado.*” [29].



**Fig. 17** The scalability of 1D and 2D DAMP over increasingly large datasets. The cost to double the number of dimensions considered is only slightly worse than double the time, suggesting that multidimensional DAMP search inherits the efficiency of the 1D version.

We have demonstrated the utility of multidimensional DAMP. However, readers may wonder if it will pay a large time overhead for it. To investigate this, we used the data shown in Fig. 15.*bottom* (wind speed) and Fig. 16 and recorded the time cost of the one-dimensional and two-dimensional algorithms for increasingly long subsets. The experimental results are shown in Fig. 17. It can be seen that the time cost of a two-dimensional DAMP is only a small constant ratio to the cost of a one-dimensional DAMP, which suggests the good scalability for multidimensional DAMP.

## 6 EMPIRICAL EVALUATION

To ensure the reproducibility of our experiments, we have built a website [10] containing all the data/code used in this work. All experiments were conducted on an Intel® Core i7-9700CPU at 3.00GHz with 32 GB of main memory, unless otherwise stated.

There are two things one normally needs to establish to validate an anomaly detection algorithm.

- **Effectiveness:** Here we feel less of an obligation. As we noted in Section 2, there are at least one hundred independent papers that have used discords to solve a real-world problem and that have shown that discords are the only technique that seems to be

able to discover anomalies that are not visually obvious (Fig. 2, Fig. 3 and Fig. 4). Nevertheless, for completeness we will show examples in Sections 6.1 and 6.2 that further demonstrate the excellent effectiveness of discords in diverse domains, and Section 6.3 and Section 6.4 offer comparisons to several deep learning-based methods.

- **Efficiency:** As this is the main contribution of the paper, here we will attempt an ambitious set of anomaly detection experiments in terms of both throughput and scale.

### 6.1 Energy Grid Dataset

Recently, a consortium from Texas A&M and USC released a large dataset on decarbonized energy grids [38]. The dataset contains files representing three years of measurements of various metrics in sixty-six electrical zones in the continental USA. As Fig. 18 suggests, each file represents eleven measurements, ten of which are *measured* (temperature, wind speed etc.), but one is *computed* from the first principles of astronomy, the Solar Zenith Angle.

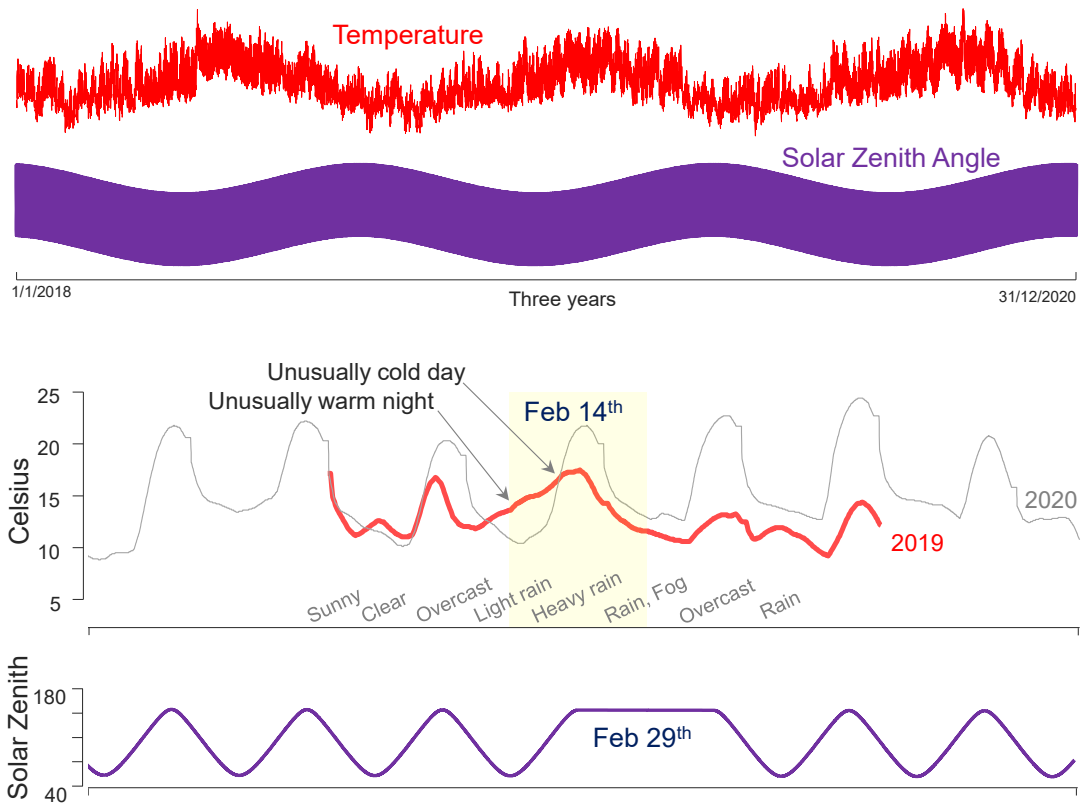


**Fig. 18** *top)* Two examples of time series from [38]. Most, like temperature are *measured*, but Solar Zenith Angle is *computed*. *bottom)* The two corresponding top discords in these datasets.

The total size of this dataset is 12 GB, representing 2,174 years of data with 1,142,668,098 datapoints. As such, we believe that it is the largest real dataset ever searched for anomalies. This complete search took only 2.06 days.

As Fig. 18 shows, most of the anomalies discovered do have a semantic meaning that can be traced. For example, a temperature trace from California had a discord that reflected “*Valentine’s Day Storm Slams California*” [33]. Even the *computed* time series reveals a strange anomaly echoing a biblical event. Joshua persuades God to stop the sun from moving for a day “*There has never been a day like it before or since* (Joshua 10:14)”. In our dataset there is a similarly unique day in which the sun apparently does not move! The reader will readily appreciate the cause of this anomaly, after noting it occurs on the 29<sup>th</sup> of February [34]. It is a classic leap year bug. Note that we informed the Texas A&M and USC team of this bug, so presumably it will be fixed in upcoming releases.

## 6.2 Machining Dataset

The example in Section 6.1 demonstrates the utility of anomaly detection in batch data exploration. However, in some cases if we can do anomaly detection in real-time, we may be able to perform an intervention to improve an outcome. For example, consider the process of making parts using a CNC milling machine. Occasionally a problem arises where an item being machined is not held correctly and it moves. This can cause a milling machine to “crash” [8]. High-end CNC mills can cost over one million dollars, and crashes resulting in more than \$20,000 in damage are known. Many (but not all) machining processes can be paused by an operator, so in principle it may be possible to stop a machine before it crashes. However, with the speed at which these machines operate, it is unlikely that the operators’ reflexes would be fast enough.

This suggests the question, could we monitor the process with telemetry, and pause the process if we detected an anomaly? In order to test this, we recreated a common scenario in Fig. 19.

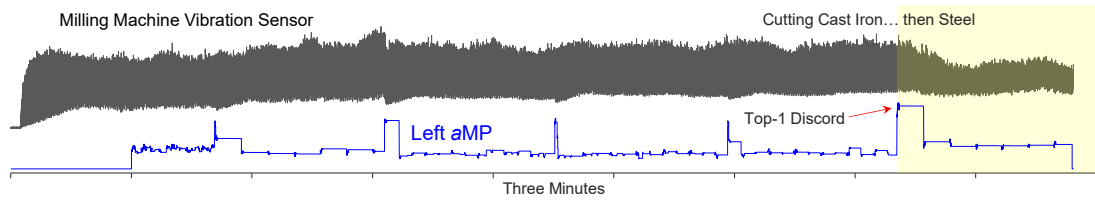


**Fig. 19** *top*) Vibration telemetry from a milling machine that was cutting cast iron, but then overshot to start cutting the steel jaws of the vice. *bottom*) The Left-*aMP* discovers the transition.

A common CNC programming error is to give the wrong coordinates for a cutting pass, and have the cutter overshoot the intended material to be machined, and inadvertently attempt to remove material from the jaws of the vice. Because the jaws are typically harder than the material they hold, and more resistant to cutting, two things can happen:

- The milling cutter itself will break. This is a \$20 to \$200 error.
- A much worse possibility is that the cutter will move the vice. If it happens to push it into the path of later traversal, this could cause a head crash, which is a \$2,000 to \$20,000 error.

As Fig. 19 shows, the *aMP* can detect the change of material, and this could be used to sound an alarm, or pause the machining process until the operator can inspect this.

Note that before the true anomaly there are other areas with high discord scores. They are when the milling cutter changes direction (from *Climb* milling to *Conventional* milling). Under our proposed scheme these would have a small cost, the process would pause until the operator visually confirms all is well, and hits *continue*.

### 6.3 Comparison to LSTM Deep Learning

Although dozens of competing deep learning anomaly detection (DLAD) algorithms now exist, it is impossible to say which is the state-of-the-art. This is because, as Wu and Keogh have demonstrated, the amount of mislabeling in the benchmark datasets dwarfs the reported differences between algorithms [35]. It makes no sense to say that algorithm **A** is 5% better than algorithm **B**, when up to 30% of the ground truth labels are suspect.

To bypass this issue, here we will compare to just *Telemanom*. It is the most cited anomaly detection paper of the last five years [14], and several independent papers have also found it to be effective. The general idea of this work is to use LSTM to predict future values, then detect anomalies based on the difference between predictions and actual data. Can *Telemanom* detect the anomalies we consider in this work?

- **ECG (Fig. 3) No.** Given the same 500 datapoint prefix as training data, it fails to find the anomaly. If we give it ten times as much training data (the first 5,000 datapoints), it *still* fails.
- **Bearing (Fig. 2): Yes.** However, *Telemanom* took a total of (517.6 training + 700.4 testing) 1,218 seconds. This is two orders of magnitude slower than DAMP, which took 16.1 seconds. More importantly, *Telemanom* is an order of magnitude slower than real-time, precluding any possibility of online monitoring.
- **Energy Grid (Section 6.1) Maybe.** There are only *objective* labels for Solar Zenith Angle (this anomaly was discovered with DAMP but *confirmed* with the data creators). If *Telemanom* sees only the first week as training data (as DAMP did), then it only learns that the Solar Zenith Angle can decrease over time, and it will flag as anomalous anything that happens after the summer solstice. A solution to this problem is to allow *Telemanom* to train on the full first year, then test on the subsequent years. Then it *may* find the “Joshua” anomaly. However, this will take 59.1 hours, over 1,300 times slower than DAMP.
- **Milling Data (Fig. 19) No.** Actually, *Telemanom* can detect the same anomaly as DAMP. But recall it can only start training when the first 5,000 datapoints arrive, and it takes 411 seconds to train the model. However, 127 seconds after it begins training, we encounter the anomaly, and about 21 seconds after that, the endmill snaps off. *Telemanom* is just too slow to be useful here.

These comparisons suggest that the most cited deep learning anomaly detection algorithm is not as accurate as DAMP, requires more training data, and is much slower.

#### 6.4 Comparison on the KDD Cup 2021 datasets

To further see the limitations of deep learning time series anomaly detection, we can compare DAMP to DLAD algorithms on publicly available benchmarks. Wu and Keogh have shown that most benchmarks in this space are too trivial to be interesting, and in any case are plagued by mislabeling and other problems [35]. Instead, we consider the KDD Cup 2021 dataset consisting of 250 univariate time series [11]. This archive was designed to be diverse, have a spectrum of difficulties ranging from easy to essentially impossible, and has a detailed provenance for each of the 250 datasets, giving us some confidence that the ground truth is correct. Moreover, the datasets



include a wide range of domains, including cardiology, industry, medicine, zoology, weather, human behavior, etc. Table 9 shows the results.

**Table 9: Accuracy and Time for Eight TSAD Methods**

Method	Accuracy	Train and Test Time
USAD [2]	0.276	8.05 hours
LSTM-VAE [27]	0.198	23.6 hours
AE [2]	0.236	6.11 hours
Telemanom [14]	<i>Out of memory error on longer examples</i>	
NORMA [4]	0.474	17.8 minutes
SCRIMP (Full-MP)	0.416	24.5 minutes
DAMP (Left-MP) out-of-the-box	0.512	4.26 hours
DAMP (Left-MP) sharpened data	0.632	4.26 hours

Once again, these results show that DAMP is more accurate and faster than deep learning-based methods. It is important to note that the results for DAMP are completely free of *any* human intervention or tuning. We use four hardcoded lines of Matlab (see [10]) to find the approximate period in each training dataset, and used that as the value of  $m$ . Likewise, we simply hardcoded a *single lookahead* value for all 250 datasets. Further optimizing the former would improve accuracy and personalizing the latter for each individual problem would improve the speed. However, we wanted to show that even the most naïve out-of-the-box use of DAMP is highly competitive. As an example of a small intervention that can further improve accuracy, if we run DAMP on *sharpened data* (a single extra line of code, see [10] for details) the accuracy improves to 0.632.

The left-discords of DAMP are significantly more accurate than the full-discords computed by SCRIMP, because some anomalies have near “twin-freaks” that suppress the distance of the anomaly to its nearest neighbor. Note that the time for SCRIMP and NORMA here is relatively good, as there are 250 *short* time series. In Fig. 22 we will see that for longer time series this advantage of SCRIMP/NORMA rapidly inverts.

We included a comparison to the recently published NORMA [4], which can be seen as a sort of Matrix Profile that uses an automatically discovered subset of the training data as the reference data. Here we used the original authors’ tools and suggestions to set the parameters (we were able to make the results *slightly* better with our own

parameter settings [10]). The time for NORMA is *apparently* good, but it is important to note the following:

- These datasets have tiny training data splits (they were deliberately made that way, to allow the deep learning community to consider them in a tenable fashion [11]). But as Fig. 23 shows the NORMA algorithm scales poorly for large datasets.
- On these datasets, we can easily close all of the time gap by using either X-Lag-Amnesic DAMP (Section 5.3.1) or Golden DAMP (Section 5.3.2), with only a minimal decrease in accuracy. Indeed, the Golden DAMP algorithm essentially subsumes NORMA as a special case.
- The results in Table 9 mask a unique timing advantage that DAMP has over not only NORMA, but all other non-trivial anomaly detectors<sup>4</sup>. We believe that DAMP is the only *instantaneous* TSAD in the literature. To see this, consider the situation in Fig. 20.

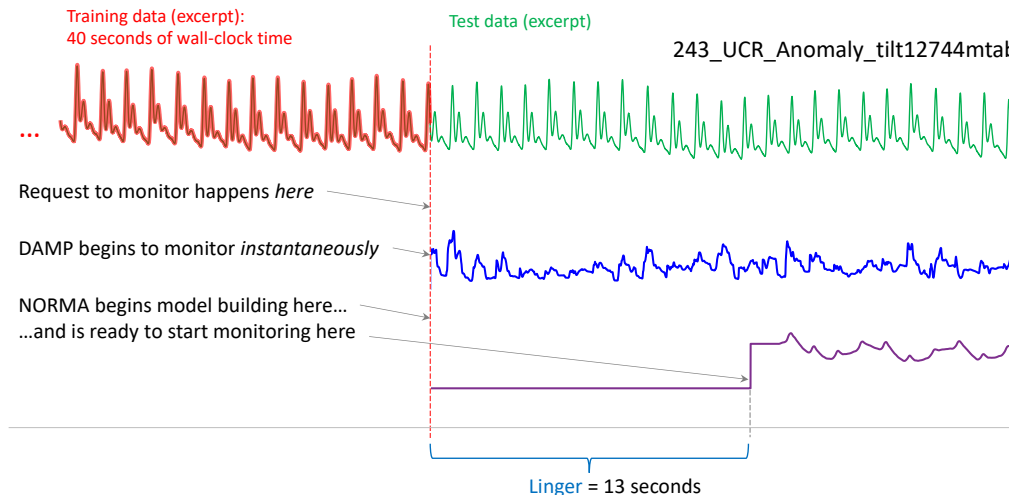


**Fig. 20** An excerpt from the 243\_UCR\_Anomaly\_tilt12744mtabledataset. The task is to exploit information in the training split, to detect the most significant anomaly in the test split. When requested, DAMP can instantaneously begin to monitor. However, NORMA (and all other TSAD algorithm), must have a period of inaction or “linger” while they build their models.

<sup>4</sup> Here we explain “non-trivial anomaly detector”. Simple rule-based conditionals such as: “**if** the time series ever reports a value that is higher than any value you have seen before, **then** flag anomaly” could be used as an anomaly detector, and could be instantaneously instantiated. By *non-trivial* we mean any TSAD algorithm that examines each subsequence for any information about shape, autocorrelation, Markov properties etc., and compares this information (in the most general sense), to a model gleaned from training data. The reader will appreciate that this includes essentially all proposed anomaly detectors in the literature.

The figure shows a dataset from the KDD Cup 2021. The first forty seconds of wall-clock time pass, and then we are invited to monitor for anomalies in the remainder of the data. We define “linger” as the time a TSAD algorithm requires to ingest the training data, build its model, and be ready to start monitoring. As shown in Fig. 20, the linger for NORMA on this problem is thirteen seconds. This means that any anomaly that occurs in the first thirteen seconds will not be detected (or will only be detected post-mortem). Note that DAMP appears to be unique among TSAD algorithms in having zero linger. In this example, the linger of NORMA may not be too consequential (although it grows rapidly with more training data, see Fig. 23). Perhaps the attending physician can wait with the patient while the model is being built. However, recall our machining example in Section 6.2. Here, if the linger is more than 127 seconds, the TSAD algorithm would not be able to avoid the expensive head-crash.

Recall that Table 9 notes “*Out of memory error on longer examples*” for *Telemanom* [8]. There does not seem to be any simple way to fix this issue, so we did the following. We sorted all the datasets from smallest to largest, and kept evaluating increasingly longer datasets until the first failure. *Telemanom* failed at the 63<sup>rd</sup> smallest dataset (114\_UCR\_Anomaly\_CIMIS44AirTemperature2). On the first 62 datasets it correctly found the anomaly on 29, giving an accuracy of 0.468. This took *Telemanom* 3.4 hours. When we run DAMP on just these 62 shorter datasets, it takes 64.9 seconds. In general, the 62 shorter test cases are the easier ones (they certainly have a much higher default rate), yet both flavors of DAMP are still significantly more accurate.

## 6.5 Threshold Learning for DAMP

Up to this point, we have experimentally demonstrated that DAMP can *locate* the most anomalous subsequence. However, we have not shown how the algorithm makes a binary decision thereafter to flag the subsequence as anomalous or not. For this purpose, we simply need to learn a *threshold*. To demonstrate, consider the following experiment. We created 200 random walk time series of length one million. As shown in Fig. 21.*top*, into half of them we randomly inserted a subtle anomaly, a low amplitude random section of length 950 (Why length 950? We found that if we used length 1,000 we got perfect accuracy, which is uninteresting for this experiment. So, we tuned the value to

give an error rate of about 10%). In Fig. 21.*left*, we show the top-1 discord score (for  $m = 1,024$ ) for all 200 time series, divided into the two cases. This plot suggests that a threshold of 36.0 is the optimal value to maximize the accuracy on future occurrences. To test this, we created and tested an additional million examples, all of which are also of length one million, classifying an actual anomaly as a true positive if the correct location of the anomaly was discovered *and* the top-1 discord score was above the threshold. Fig. 21.*right* shows the confusion matrix.

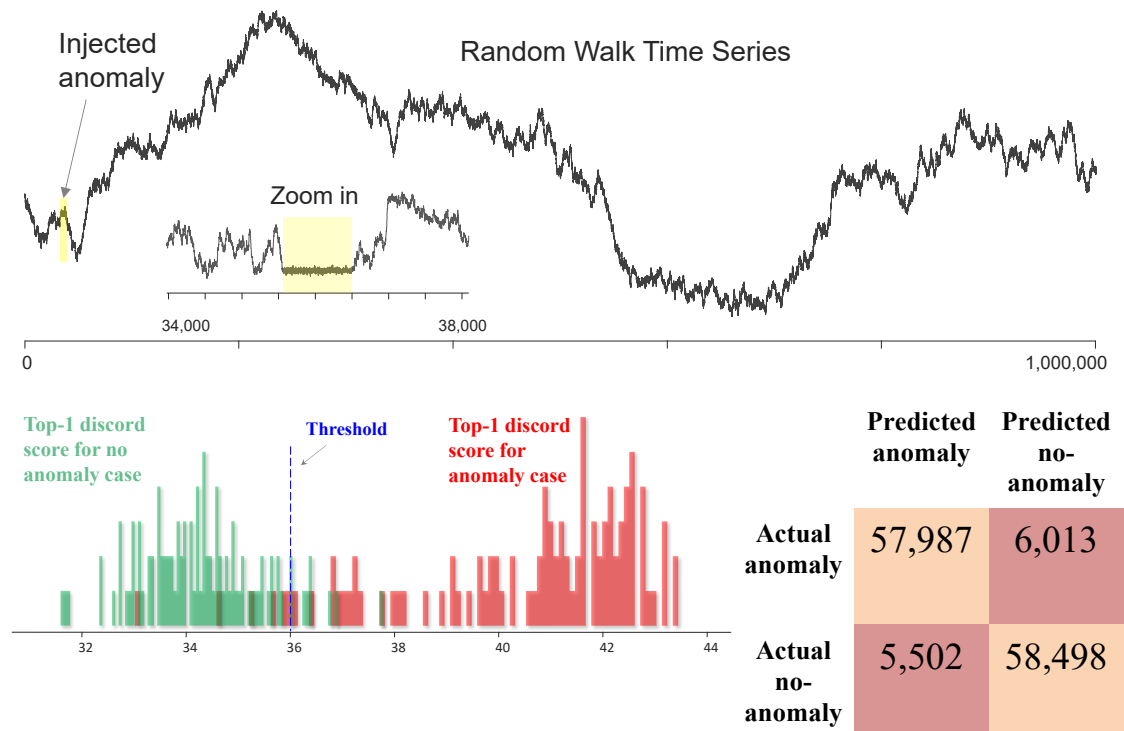


**Fig. 21** *top*) A sample random walk with an anomaly embedded. *left*) The distribution of top-1 discord scores for the two cases of interest. *right*) The confusion matrix for this task.

We note in passing that this experiment (which took several days distributed across commodity laptops and desktops), trained on time series with a total length of 200 million, and tested on time series with a total length of 128 billion. To the best of our knowledge, this is the largest scale time series anomaly detection experiment ever conducted. Could deep learning do this? We estimate that *Telemanom* [14] would take about twelve years to do this, although in practice it gives *out-of-memory* errors.

## 6.6 Scalability Comparisons

To find out which elements of our proposed method contribute most to its efficiency, we have performed an ablation study, in which various elements of DAMP were progressively crippled. As a baseline, we also compare to SCRIMP [39]. This

comparison to SCRIMP is a little unfair, as it discovers motifs as well as discords. However, it seems to be the most used discord discovery algorithm in recent years. Fig. 22 summarizes our findings.

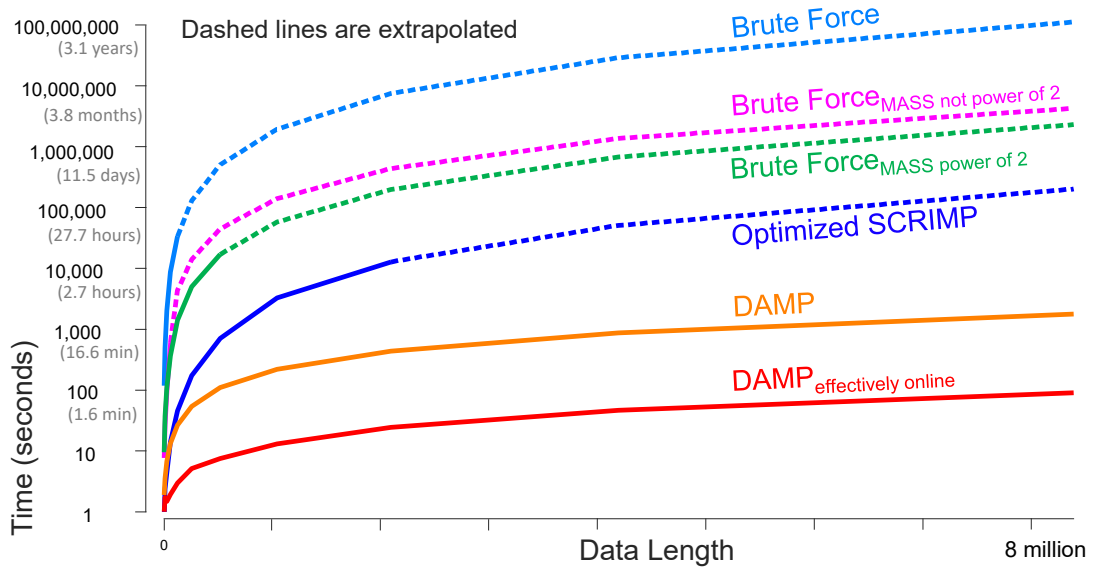


**Fig. 22** The CPU time vs time series length for various discord discovery algorithms. Note the Y-axis is in log scale.

It is clear that each element we proposed does actually contribute to speed up, and that DAMP is effectively linear in  $n$ .

As we earlier noted, most of the benchmark datasets are only hundreds to thousands of datapoints long [35], and that seems to have set the limit of the ambition of most of the community when it comes to scalability. However, a recent paper pushed that envelope by considering a two million length ECG dataset [4]. In fact, these authors graciously gave us the *exact* dataset they used, (which was in fact even longer than they considered in [4]), and helped us create a perfectly commensurate experiment, as shown in Fig. 23. A real-time video trace of this experiment is at [10].



**Fig. 23** (Most of this figure is taken from [4] with permission, only the green elements are new). The scalability of various algorithms on increasing large subsets of a long ECG trace. All algorithms except DAMP are limited to the first 2M data points by [4]. Note that the Y-axis is logarithmic.

Note that of the many approaches considered, some time out (i.e., are not finished in a four-hour cutoff) at length 500K. In contrast, DAMP can handle eight million datapoints in just 22.3 seconds, this is over 358,000 Hz. In fact, DAMP is so fast, that the time it reports for the 50K length trial is literally off the original chart, taking less than one second.

As eight million datapoints are about the longest publicly available ECG, in Fig. 24 we conclude this section by searching a single random walk time series of length  $2^{30}$ .

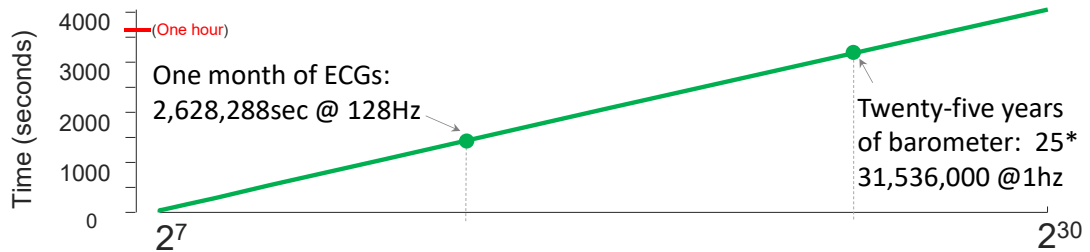


**Fig. 24** The time taken for DAMP to process a random walk time series of length  $2^{30}$  (just over one billion). For context, we have labeled the size of two concrete tasks, processing a month of ECGs and twenty-five years of sensor data.

## 6.7 Scalability and Stability of DAMP

One of Wu and Keogh's criticisms of common benchmarks is *unrealistic anomaly density* [35]. They noted that over 20% of the data is labeled anomalous in many benchmarks, which poses a real problem for the evaluation. Suppose that an algorithm has near perfect sensitivity, but it will randomly give out a false positive once in every million datapoints (perhaps due to the numerical instability of streaming algorithms [13]). Note that because most benchmarks in the literature only have a few thousand datapoints, this issue would almost certainly not be observed during testing. However, it clearly would be a problem for any real-world deployment. For example, for a continuous processing system with telemetry reporting every second, this would give us about thirty-one false positives a year.

To demonstrate DAMP does not have this issue, we did the following test. Recall the subtle anomaly shown in the 100,000 datapoint MGAB dataset in Fig. 4. We can append anomaly-free data from the same Mackey-Glass model (but free of the embedded anomalies [31]) to make it one thousand times longer, i.e., a total length of 100 million. When we search this with DAMP ( $m = 40$ ), we count a trial successful if the top-1 discord is found in the first 100,000 datapoints (created by [31]), rather than from the

appended ninety-nine million nine hundred thousand datapoints. Each of the coauthors of this work ran this experiment multiple times in the background of their desktops over a week, and in total conducted over 16,000 such trials, finding a total of zero false positives.

Note that this experiment required performing anomaly detection on time series with a total length of 1.648 trillion datapoints, using off-the-shelf hardware. This is something that would be inconceivable with any other anomaly detection method.

## **7 CONCLUSIONS AND FUTURE WORK**

In this paper, we created the left-discord anomaly detection framework, generalizing classic time series discords that previously only handled the batch case, to the online case, and solving the twin-freak problem in the process. Further, we have introduced DAMP, a fast and scalable algorithm to discover such discords. Experimental results have demonstrated that our proposed left-discords outperform the current SOTA methods, including the most cited deep learning methods in terms of accuracy. Moreover, we have further demonstrated that DAMP is orders of magnitude faster and more scalable than any method in the literature.

We believe that the throughput and scalability of DAMP will allow the community to address datasets and applications that are currently out of reach, and that this will open new challenges and research problems. Finally, we have made all our code and data available to the community to confirm and build upon our work.

## **8 ACKNOWLEDGMENTS**

This research was supported by NSF OIA-1757207, CNS-2008910 and RI-2104537, the French National Research Agency (ANR-19-P3IA-0002), and NSF 2103976, Mitsubishi, Visa and Toyota. We sincerely thank the authors of [4] for their help in creating Fig. 23.

## **9 REFERENCES**

- [1] Aubet F-X, Zügner D, Gasthaus J (2021) Monte Carlo EM for Deep Time Series Anomaly Detection. arXiv:2112.14436 [cs, stat]
- [2] Audibert J, Marti S, Guyard F, Zuluaga MA (2021) From Univariate to Multivariate Time Series Anomaly Detection with Non-Local Information. In: Lemaire V, Malinowski S, Bagnall A, et al. (eds) *Advanced Analytics and Learning on Temporal Data*. Springer International Publishing, Cham, pp 186–194
- [3] Batista GEAPA, Keogh EJ, Tataw OM, de Souza VMA (2014) CID: an efficient complexity-invariant distance for time series. *Data Min Knowl Disc* 28:634–669. <https://doi.org/10.1007/s10618-013-0312-3>

- [4] Boniol P, Linardi M, Roncallo F, et al (2021) Unsupervised and scalable subsequence anomaly detection in large data series. *The VLDB Journal* 30:909–931. <https://doi.org/10.1007/s00778-021-00655-8>
- [5] Boniol P, Paparrizos J, Palpanas T, Franklin MJ (2021) SAND: streaming subsequence anomaly detection. *Proceedings of the VLDB Endowment* 14:1717–1729
- [6] Bu Y, Chen L, Fu AW-C, Liu D (2009) Efficient anomaly monitoring over moving object trajectory streams. In: *Proceedings of the 15th ACM SIGKDD international conference on Knowledge discovery and data mining - KDD '09*. ACM Press, Paris, France, p 159
- [7] Case Western Reserve University Bearing Data Center. [Online]. Available: <https://csegroups.case.edu/bearingdatacenter/home>. Accessed: Nov. 15, 2021.
- [8] CNC Crashes. Video. (15 Feb 2018). from <https://youtu.be/t2tBtZCa7j4?t=205>. Retrieved December 20, 2021.
- [9] Daigavane A, Wagstaff KL, Doran G, et al (2022) Unsupervised detection of Saturn magnetic field boundary crossings from plasma spectrometer data. *Computers & Geosciences* 161:105040
- [10] DAMP (2022) <https://sites.google.com/view/discord-aware-matrix-profile>
- [11] Dau HA, Bagnall A, Kamgar K, et al (2019) The UCR time series archive. *IEEE/CAA J Autom Sinica* 6:1293–1305. <https://doi.org/10.1109/JAS.2019.1911747>
- [12] Doshi K, Abudalou S, Yilmaz Y (2022) TiSAT: Time Series Anomaly Transformer. arXiv:220305167 [cs, eess, stat]
- [13] Higham NJ (2002) *Accuracy and Stability of Numerical Algorithms* (2 ed). ISBN: 978-0-89871-521-7
- [14] Hundman K, Constantinou V, Laporte C, et al (2018) Detecting Spacecraft Anomalies Using LSTMs and Nonparametric Dynamic Thresholding. In: *Proceedings of the 24th ACM SIGKDD International Conference on Knowledge Discovery & Data Mining*. ACM, London United Kingdom, pp 387–395
- [15] Imani S, Madrid F, Ding W, et al (2020) Introducing time series snippets: a new primitive for summarizing long time series. *Data Min Knowl Disc* 34:1713–1743. <https://doi.org/10.1007/s10618-020-00702-y>
- [16] Keogh E (2021) Irrational Exuberance Why we should not believe 95% of papers on Time Series Anomaly Detection. 7th SIGKDD Workshop on Mining and Learning from Time Series at SIGKDD 2021. Workshop Keynote <https://www.youtube.com/watch?v=Vg1p3DouX8w&t=324s>
- [17] Khansa HE, Gervet C and Brouillet A (2012) Prominent Discord Discovery with Matrix Profile : Application to Climate Data Insight. 10th International Conference of Advanced Computer Science & Information Technology (ACSIT 2022) May 21–22, 2022, Zurich, Switzerland
- [18] Kirti R, Karadi R (2012) Cardiac tamponade: atypical presentations after cardiac surgery. *Acute Medicine* 11:93–96
- [19] Mueen A, Zhu Y, Yeh M, et al (2017) The fastest similarity search algorithm for time series subsequences under euclidean distance. url: [www.cs.unm.edu/~mueen/FastestSimilaritySearch.html](http://www.cs.unm.edu/~mueen/FastestSimilaritySearch.html). Accessed 24 January, 2022
- [20] Murray D, Liao J, Stankovic L, et al A data management platform for personalised real-time energy feedback.
- [21] Nakamura T, Imamura M, Mercer R, Keogh E (2020) MERLIN: Parameter-Free Discovery of Arbitrary Length Anomalies in Massive Time Series Archives. In: *2020 IEEE International Conference on Data Mining (ICDM)*. IEEE, Sorrento, Italy, pp 1190–1195
- [22] National Weather Service. *January 24, 2019 Heavy Rain and Flooding*. from <https://www.weather.gov/aly/24Jan19HeavyRainFlood>. Retrieved May 1 2022.
- [23] Neupane D, Seok J (2020) Bearing Fault Detection and Diagnosis Using Case Western Reserve University Dataset With Deep Learning Approaches: A Review. *IEEE Access* 8:93155–93178. <https://doi.org/10.1109/ACCESS.2020.2990528>
- [24] Nilsson F (2022) Joint Human-Machine Exploration of Industrial Time Series Using the Matrix Profile. Halmstad University, School of Information Technology, Halmstad Embedded and Intelligent Systems Research (EIS), CAISR - Center for Applied Intelligent Systems Research.
- [25] Palpanas T. Personal communication June 4<sup>th</sup> 2022.
- [26] Paparrizos J, Kang Y, Boniol P, et al (2022) TSB-UAD: An End-to-End Benchmark Suite for Univariate Time-Series Anomaly Detection. *Proceedings of the VLDB Endowment (PVLDB) Journal*
- [27] Park D, Hoshi Y, Kemp CC (2018) A Multimodal Anomaly Detector for Robot-Assisted Feeding Using an LSTM-Based Variational Autoencoder. *IEEE Robot Autom Lett* 3:1544–1551. <https://doi.org/10.1109/LRA.2018.2801475>
- [28] Park JY, Wilson E, Parker A, Nagy Z (2020) The good, the bad, and the ugly: Data-driven load profile discord identification in a large building portfolio. *Energy and Buildings* 215:109892
- [29] Silive.com. *Wild storm pelts Staten Island with giant hail -- 'threat of tornado has passed'* from <https://www.silive.com/news/2019/05/nws-issues-tornado-warning-for-staten-island.html>. Retrieved May 1 2022.
- [30] Su Y, Zhao Y, Niu C, et al (2019) Robust anomaly detection for multivariate time series through stochastic recurrent neural network. pp 2828–2837
- [31] Thill M, Konen W, Bäck T (2020) *Time series encodings with temporal convolutional networks*. Springer, pp 161–173



- [32] Truong HT, Ta BP, Le QA, et al (2022) Light-weight federated learning-based anomaly detection for time-series data in industrial control systems. *Computers in Industry* 140:103692. <https://doi.org/10.1016/j.compind.2022.103692>
- [33] Wastewater News. *Valentine's Day Storm Slams California, Pushing Water Agencies to the Edge*. from [www.news.cornell.edu/Chronicle/00/5.18.00/wireless\\_class.html](http://www.news.cornell.edu/Chronicle/00/5.18.00/wireless_class.html). Retrieved Dec 1 2021.
- [34] Wikipedia. Leap year problem. from [https://en.wikipedia.org/wiki/Leap\\_year\\_problem](https://en.wikipedia.org/wiki/Leap_year_problem). Retrieved December 1, 2021.
- [35] Wu R, Keogh E (2021) Current Time Series Anomaly Detection Benchmarks are Flawed and are Creating the Illusion of Progress. *IEEE Trans Knowl Data Eng* 1–1. <https://doi.org/10.1109/TKDE.2021.3112126>
- [36] Yeh C-CM, Zheng Y, Wang J, et al (2021) Error-bounded Approximate Time Series Joins using Compact Dictionary Representations of Time Series. *CoRR abs/2112.12965* (2021)
- [37] Yeh C-CM, Zhu Y, Dau HA, et al (2019) Online amnesic dtw to allow real-time golden batch monitoring. pp 2604–2612
- [38] Zheng X, Xu N, Trinh L, et al (2021) PSML: A Multi-scale Time-series Dataset for Machine Learning in Decarbonized Energy Grids. *arXiv preprint arXiv:211006324*
- [39] Zhu Y, Yeh C-CM, Zimmerman Z, et al (2018) Matrix profile XI: SCRIMP++: time series motif discovery at interactive speeds. *IEEE*, pp 837–846